

Intraplate earthquakes and the state of stress in oceanic lithosphere

ERIC A. BERGMAN

Department of Earth, Atmospheric, and Planetary Sciences, Massachusetts Institute of Technology, Cambridge, MA 02139 (U.S.A.)

(Received October 2, 1985; accepted February 17, 1986)

Abstract

Bergman, E.A., 1986. Intraplate earthquakes and the state of stress in oceanic lithosphere. In: B. Johnson and A.W. Bally (Editors), *Intraplate Deformation: Characteristics, Processes and Causes*. *Tectonophysics*, 132: 1–35.

The sources of stress responsible for oceanic intraplate earthquakes and their usefulness for inferring the tectonic stress field are investigated through a synthesis of the source mechanisms of 58 of the largest such events, determined by inversion of long-period P and SH waveforms. Further constraints are provided by the global distribution of oceanic intraplate seismicity and a calculation of the seismic moment release per unit volume of seismogenic lithosphere as a function of lithosphere age. Although frequently associated with relict tectonic features, large oceanic intraplate earthquakes are generally reliable indicators of the state of stress in the source region. Most oceanic intraplate seismicity occurs in young lithosphere (< 35 m.y. old) and appears to be dominated by stresses related to the early evolution of oceanic lithosphere, particularly thermoelastic stresses. Consequently, these events are a poor source of information about plate driving forces. Large earthquakes in old oceanic lithosphere tend to be concentrated in a few regions undergoing significant intraplate deformation, which in some cases appear to be related to abnormally high levels of stress and in others can be characterized as diffuse, incipient, or reactivated plate boundaries. The state of stress inferred from such events is often related in a fundamental way to the forces driving plate motions. The rarity of large earthquakes in many old ocean basins is attributed to the capacity of old oceanic lithosphere to support a compressive stress comparable in magnitude to that due to elevated topography at spreading ridges, the source of the ambient tectonic stress field in most such regions.

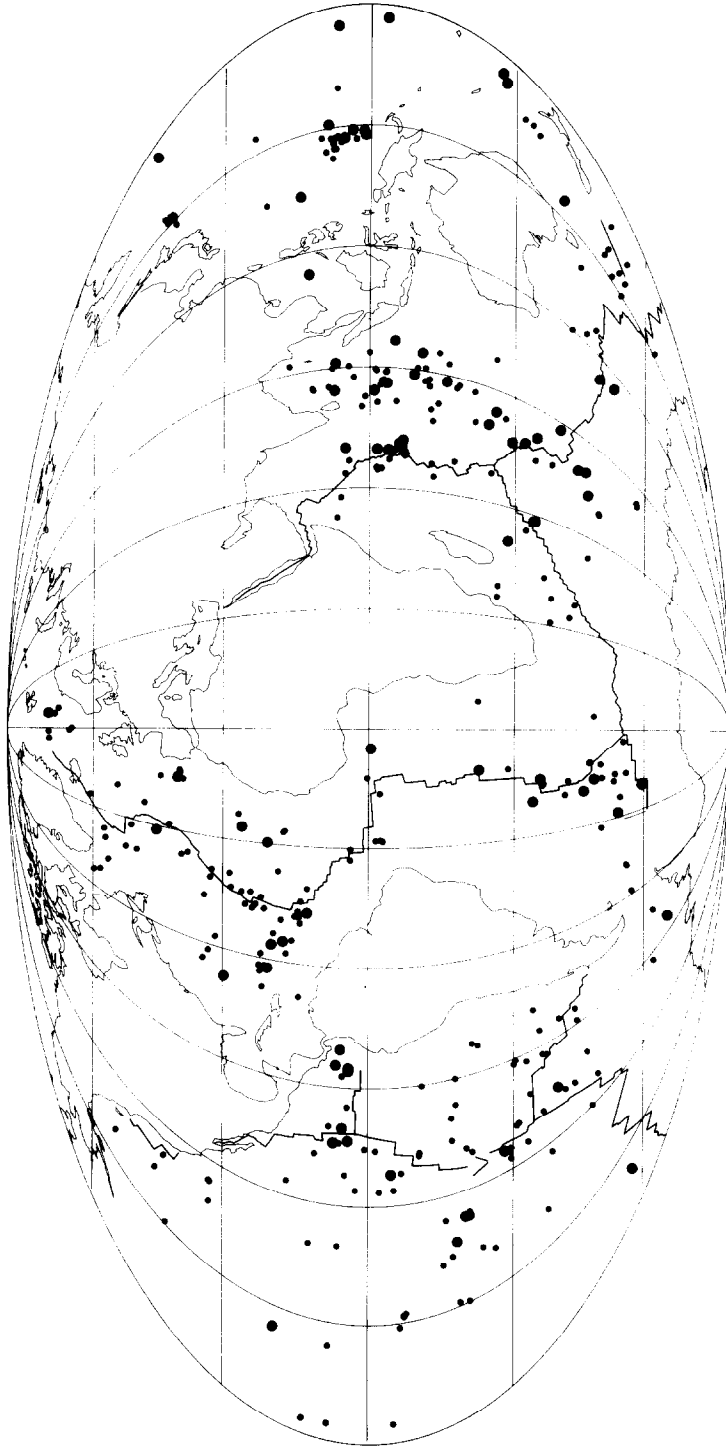
Introduction

A small percentage of teleseismically-detected earthquakes are located away from the boundaries of the major plates. These “intraplate” earthquakes are largely ignored in first-order plate tectonics, which is simply a kinematic description of perfectly rigid lithospheric plates. However, as the focus of research has shifted to the dynamics of plate motions and the non-rigid behavior of the lithosphere, intraplate earthquakes have attained an importance far out of proportion to their number. This is because such earthquakes are a primary source of information on the extent and character of intraplate deformation. They may also serve to delineate the intraplate stress field, which is

thought to reflect the distribution of plate boundary forces, i.e., the driving mechanism of plate tectonics.

The purpose of this paper is to elaborate a hypothesis concerning the relationship between intraplate earthquakes and the state of stress in oceanic lithosphere, one which addresses in particular two questions: (1) How reliable are earthquakes as indicators of stress orientation, and (2) What are the dominant sources of stress relieved in oceanic intraplate earthquakes?

The primary data for this investigation are detailed source studies of 58 of the largest oceanic intraplate earthquakes, performed with a body-waveform inversion technique developed by Nabelek (1984). The results for 43 of the events



OCEANIC INTRAPLATE EARTHQUAKES 1964–1983

Fig. 1. Global distribution of epicenters of oceanic intraplate earthquakes occurring from January 1, 1964 through 1983, based on the compilation of Bergman (1984). Earthquakes with $m_b \geq 5.4$ are indicated by larger symbols. Mollweide projection, centered at 0° longitude. Major oceanic spreading centers are approximately indicated by solid lines.

TABLE 1

Epicentral data ^a and source parameters for earthquakes studied

Mo/Da/Yr	Origin time			Lat. °N	Long. °E	m_b	M_s	Age ^b (m.y.)	M_0 ^c	Depth ^d	Mechanism ^e
	h	m	s								
10/23/64	1	56	5.1	19.80	-56.11	6.2	6.3	65	52.	28	285/56/152
10/07/65	3	36	1.4	12.46	114.45	5.8	5.6	17-32	5.5	3	218/43/083
08/20/68	11	16	58.5	5.43	147.11	5.6	5.0	32	5.3	6	126/54/035
09/03/68	15	37	0.3	20.58	-62.30	5.6	5.9	80	6.6	25	168/76/004
09/30/71	21	24	10.8	-0.45	-4.89	6.0	5.5	46	11.	12	079/60/074
05/21/72	6	1	54.3	-27.10	174.97	5.6	4.9	28	4.7	13	333/71/157
10/20/72	4	33	49.9	20.60	-29.69	5.7	5.8	90	27.	18	250/79/169
04/26/73	20	26	27	20.05	-155.16	5.9	5.9	90	46.	45	083/59/347
04/12/74	17	45	18.7	14.27	134.37	5.5	4.9	35	1.2	11	072/53/071
11/20/74	13	21	41.6	-53.59	-28.26	5.8	5.6	70	7.2	11	333/46/069
08/30/76	8	37	54.4	1.03	147.56	5.8	5.9	34	25.	26	332/76/172
02/05/77	3	29	19	-66.49	-82.45	6.1	6.2	53	39.	15	002/42/073
10/17/77	17	26	40.4	-27.93	173.13	6.2	6.7	28-35	200.	13	274/78/009
12/13/77	1	14	20.5	17.33	-54.91	5.7	6.4	68	45.	20	238/60/049
03/24/78	0	42	36.7	29.68	-67.45	6.0	6.0	118	22.	8	330/44/089

^a Epicentral data from the ISC, except M_s , magnitudes for October 23, 1964 (Stein et al., 1982), October 7, 1965 (Wang et al., 1979), and September 3, 1968 (Wiens and Stein, 1983).

^b Lithospheric age estimated from magnetic anomaly identifications and magnetic chronology of LaBrecque et al. (1977), or from the isochrons determined by Selater et al. (1980, 1981).

^c Seismic moment in units of 10^{24} dyn cm (10^{17} N m).

^d km below seafloor.

^e Strike/dip/slip, convention of Aki and Richards (1980).

have been reported previously (Bergman et al., 1984; 1985; Bergman and Solomon, 1984; 1985). The appendix contains the details of the source studies for the remaining 15 events, which occurred in older lithosphere in the Atlantic and Pacific Oceans. The source parameters are listed in Table 1. Interpretations of these source studies in terms of local and regional tectonic problems are presented below.

Moment-magnitude relations derived from all 58 source studies are combined with the catalog of oceanic intraplate earthquakes of Bergman (1984) to estimate seismic moment release per unit volume of seismogenic lithosphere as a function of lithosphere age. The high concentration of seismic moment release in young oceanic lithosphere, a pattern previously noted by Wiens and Stein (1983), provides an important clue to understanding the dominant sources of stress resulting in oceanic intraplate seismicity.

For the purpose of gaining a global perspective on the relationship between intraplate earthquakes and the state of stress in the oceanic lithosphere,

we take as data the source parameters (particularly their variations with respect to depth and lithospheric age) and local or regional tectonic associations of the largest oceanic intraplate earthquakes, the general pattern of seismic moment release, and the geographic distribution of epicenters of oceanic intraplate earthquakes of all sizes (Fig. 1).

Intraplate earthquakes in the Atlantic Ocean

The local and regional tectonic significance of seven earthquakes in older lithosphere in the Atlantic Ocean is discussed in this section. Six of the events are in the North Atlantic; the seventh is located in the far South Atlantic, near the South Sandwich Arc. There have been no significant intraplate earthquakes in older oceanic lithosphere of the main South Atlantic basin since the establishment of the World Wide Standard Seismograph Network (WWSSN) in the early 1960's.

These earthquakes can be grouped, for the purpose of discussion, into three categories: (1) iso-

lated events unrelated to major intraplate deformation; (2) events belonging to a diffuse zone of intraplate seismicity which may be associated with a distributed plate boundary; (3) intraplate earthquakes in the vicinity of a complex plate boundary which may strongly influence the local intraplate stress field. In the first category we place the September 30, 1971 (Guinea Basin), October 20, 1972 (Cape Verde), and March 24, 1978 (Bermuda) earthquakes. The second category includes the events on October 23, 1964, September 3, 1968, and December 13, 1977, between the Caribbean Arc and the Mid-Atlantic Ridge. The earthquake on November 20, 1974, in the vicinity of the South Sandwich Arc, belongs to the third category.

Isolated events

The epicenter of the September 30, 1971 earthquake is in the equatorial eastern Atlantic, in the Guinea Basin (Fig. 2). There are numerous closely-spaced fracture zones, trending approximately N75°E, throughout the region, but none has been identified in the immediate epicentral area (Sibuet and Mascle, 1978). There are distinct linear trends in the bathymetry, however. One nodal plane of the thrust-faulting focal mechanism is subparallel to the local trend of fracture zones.

The October 20, 1972 event is located northwest of the Cape Verde Archipelago in the eastern Atlantic (Fig. 3). Although the epicentral region is poorly surveyed, the tectonic history of this region is thought to be reasonably simple and fracture

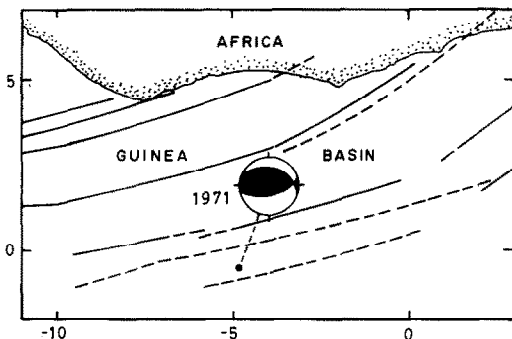


Fig. 2. Major fracture zones (dashed where less certain) in the Guinea Basin and the location and mechanism of the September 30, 1971 earthquake. Adapted from fig. 8 of Sibuet and Mascle (1978).

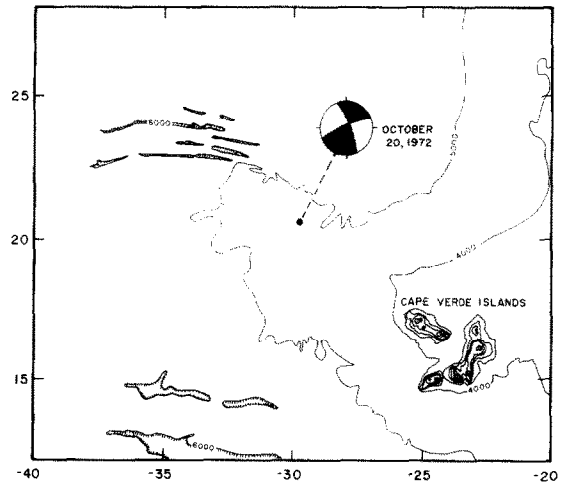


Fig. 3. Bathymetry in the vicinity of the Cape Verde Rise in the eastern Atlantic and the epicenter and focal mechanism of the October 20, 1972 earthquake. Bathymetry from Perry et al. (1981); 1000 m contour interval.

zones are expected to trend WNW. The strike-slip focal mechanism is very well constrained in the body waveform inversion, but neither nodal plane is close to the trend of fracture zones.

The epicenter of the thrust-faulting March 24, 1978 earthquake is 375 km southwest of Bermuda in the western Atlantic, at the edge of the uplifted Bermuda platform and in the middle of the M11–M4 spreading discontinuity (Fig. 4). The strike of fracture zones changes from about 300° (on the east) to about 290° in the epicentral region, but the epicenter itself is not associated with a fracture zone.

Both the September 30, 1971 and March 24, 1978 events are probably associated with disturbed lithosphere. The 1971 Guinea Basin earthquake almost certainly occurred on a fracture zone. Fracture zones in the vicinity of the 1978 Bermuda earthquake are well-mapped and the epicenter clearly lies between fracture zones, but the Mesozoic spreading discontinuity in the epicentral region likely coincides with a significant disturbance of the lithosphere (Fig. 4).

Because of its location in a well-surveyed part of the western Atlantic and the microaftershock survey of Nishenko et al. (1982), more is known about the circumstances of the 1978 Bermuda event than almost any other oceanic intraplate event, yet the source of the stress released in this

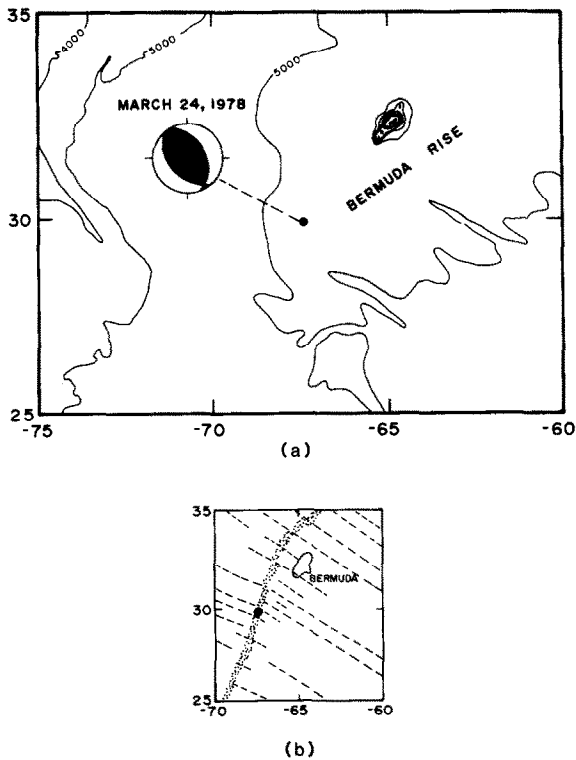


Fig. 4. (a) Bathymetry in the vicinity of the Bermuda Rise, in the eastern Atlantic, and the location and focal mechanism of the March 24, 1978 earthquake. Bathymetry from Perry et al. (1981); 1000 m contour interval. (b) Locations of fracture zones and the M11-M4 spreading discontinuity (stippled region) in the epicentral region of the March 24, 1978 earthquake (solid circle). Adapted from Fig. 9 of Nishenko and Kafka (1982).

event has not been clearly identified. The P -axis is oriented radially to the island of Bermuda, but the epicenter is too far away for the mechanism to be explained by simple topographic effects. Plate bending stresses resulting from a large seamount load can be significant at greater distances, but the shallow depth and thrust-faulting mechanism are inconsistent with such a model. Nishenko and Kafka (1982) argue that the 1978 Bermuda earthquake may have released stresses related to crustal thickness inhomogeneities at the perimeter of the Bermuda Rise. Alternatively, basal drag forces could be invoked, because the P -axis is subparallel to the absolute motion vector of the North American plate determined by Minster and Jordan (1978). The orientation of the P -axis is also consistent with the orientation of maximum horizon-

tal compressive stress predicted by a finite element model of the intraplate stress field incorporating "ridge push" and basal drag forces on the plates (Richardson et al., 1979).

The 1972 Cape Verde earthquake occurred near the perimeter of the Cape Verde Rise, but the P -axis is subparallel to the presumed gradient in crustal thickness. There is no significant topographic relief in the area. The 1971 Guinea Basin earthquake has a thrust-faulting mechanism with the P -axis roughly perpendicular to the continental margin of Africa to the north, but the margin is too distant (300–400 km) for it to be a significant source of stress. There is thus no obvious reason to reject these two events as indicators of the regional stress field in the African plate.

A diffuse plate boundary?

Several of the larger oceanic intraplate earthquakes in the western Atlantic have occurred between the Caribbean Arc and the Mid-Atlantic Ridge (MAR), an area in which any relative motion between the North and South American plates should occur (e.g., Ball and Harrison, 1970). Bergman and Solomon (1980) and Stein et al. (1982) found no clear relation, however, between the mechanisms of several of these events and a postulated plate boundary.

Further insight to this question can be gained by considering the distribution of intraplate seismicity at magnitudes below that necessary for a teleseismic source study. Figure 1 reveals a diffuse, but distinct band of earthquake activity extending SE from the northern end of the Lesser Antilles to the MAR. This seismicity pattern was also noticed by Lilwall (1982). This region is shown in more detail in Fig. 5, with the focal mechanisms determined for the largest events. Only events recorded at 10 or more stations are shown; the diffuse band of seismicity between the MAR and the northern end of the Caribbean Arc is even more prominent if events recorded at fewer than 10 stations are plotted.

This diffuse band of intraplate seismicity intersects the MAR in a region where it undergoes a major left-lateral offset, involving several transform faults. The general trend of the intraplate

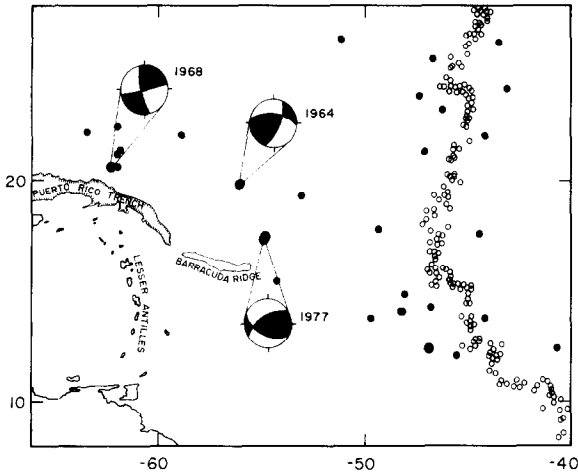


Fig. 5. Map of the seismicity of a portion of the western Atlantic, with focal mechanisms for three earthquakes determined by inversion of body waveforms (October 23, 1964, September 3, 1968, and December 13, 1977). Oceanic intraplate earthquakes are shown as solid circles, with larger symbols for events with $m_b \geq 5.4$. Small open circles indicate the seismicity of the Mid-Atlantic Ridge. Earthquakes in the Lesser Antilles Arc are not shown. The Puerto Rico Trench (outlined by the 6000 m isobath) and the Barracuda Ridge (5000 m isobath) are also shown.

seismicity is also roughly parallel to fracture zones in the area. The average width (350 km) and trend ($N63^\circ W$) of the pattern of intraplate seismicity in this region may be largely controlled by numerous closely-spaced fracture zones with significant offset.

The focal mechanisms of the October 1964 and the December 1977 earthquakes (Fig. 5) both have a nodal plane subparallel to the local trend of fracture zones, approximately WNW. A 1978 event very near the 1977 earthquake was found by Stein et al. (1982) to have a very similar mechanism. If we take these nodal planes to represent the fault planes, all three events are characterized by a combination of thrust and right-lateral strike-slip faulting. The September 1968 event has a similar mechanism, but the nodal plane differs in strike by about 25° from the general trend of fracture zones. This difference may be attributed to perturbations in the stress field in the vicinity of the Puerto Rico Trench.

Right-lateral motion on a plane striking WNW is predicted by relative plate motion model RM2 (Minster and Jordan, 1978), whereas model RM1

(Minster et al., 1974) predicts left-lateral motion. RM2 predicts a small component of extension across a boundary oriented $N63^\circ W$ at $19^\circ N$, $55^\circ W$, however, where the earthquake data require compression. The pole determined by Chase (1978) predicts slow compression across the boundary, but very little transverse motion. The error ellipse for this pole of rotation (both in RM2 and Chase's model) is quite large and would easily accommodate the shift necessary to place the proposed diffuse North America–South America boundary in compression.

Complex local tectonics

The November 20, 1974 earthquake is located about 150 km north of the South Sandwich Arc, in a poorly surveyed area (Fig. 6). The South American plate is being deformed in a complex manner as the South Sandwich Arc propagates east at the full spreading rate of the Scotia Ridge (70–90 mm/yr), shearing off and subducting a strip of the South American plate (Barker, 1972; Forsyth, 1975). Considering the seismic quiescence of older oceanic lithosphere in the South Atlantic,

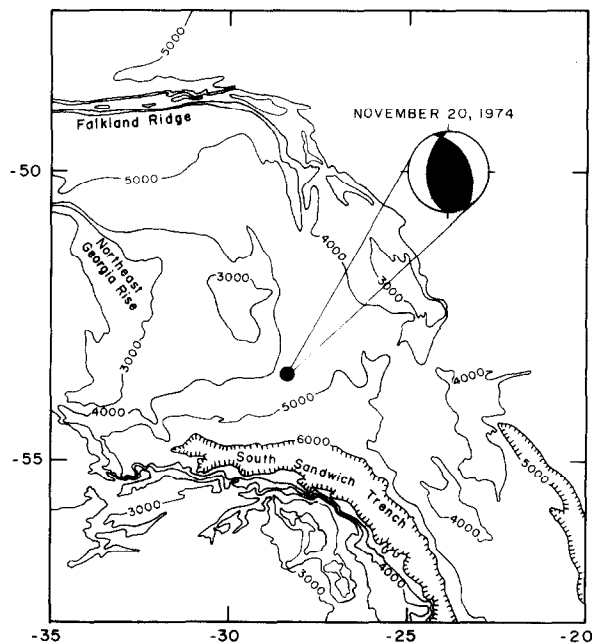


Fig. 6. Bathymetry north of the South Sandwich Arc and the epicenter and focal mechanism of the November 20, 1974 earthquake. Selected isobaths from LaBrecque and Rabinowitz (1981).

except in the vicinity of the South Sandwich Arc, it is quite likely that this event relieved stresses predominantly of local origin. The epicenter is near the base of the Northeast Georgia Rise and the nodal planes are subparallel to its edge. Although the P -axis of this event is roughly perpendicular to the margin of the rise, local topographic stresses are unlikely to be a significant factor in this earthquake (centroid 11 km beneath the seafloor), since such stresses are largest at shallow depth. A boundary fault along the edge of the platform may have been reactivated in this earthquake, however.

Intraplate earthquakes in the Pacific Ocean

In this section, I discuss the local and regional tectonic significance of eight earthquakes in older oceanic lithosphere of the Pacific Basin and in several marginal basins. The most striking feature of seismicity in old lithosphere of the Pacific plate is its absence. Aside from Hawaii, the major sites of intraplate seismicity in the western Pacific are the Gilbert Islands and the eastern Caroline Islands. I studied one Hawaiian event, the Hilo earthquake on April 26, 1973, and two earthquakes in the eastern Caroline Islands. Lay and Okal (1983) made an extensive study of the highly unusual Gilbert Islands swarm of 1981–1983. The South China Sea, Philippine Sea, and South Fiji Basin (two events) have all experienced intraplate earthquakes large enough for the long-period body waves to be modeled. One large event in older lithosphere of the Antarctic plate in the southeastern Pacific has also been investigated.

Caroline Islands

A variety of geophysical evidence indicates that lithosphere in the East and West Caroline basins at one time constituted a separate plate, but that it subsequently became attached to the Pacific plate (e.g., Bracey, 1975; Mammerickx, 1978; Weissel and Anderson, 1978). Although deformation may have re-occurred recently around the northern and eastern margins of the former Caroline plate, it is not clear that a true plate boundary has again developed. Hegarty et al. (1983) suggest that the

northern and eastern boundaries of the plate have been active only since about 1 m.y.B.P. The seismicity of the area, while high by intraplate standards, is diffuse and for the most part not clearly associated with the proposed plate boundaries.

The August 20, 1968 earthquake is one of the few events which does seem to be directly associated with one of the zones of deformation proposed as an incipient plate boundary (Fig. 7). The epicenter is in a transitional part of the boundary: To the south, the deformation is expected to be mainly compressional across the Mussau Trough, while along the Sorol Trough to the west, left-lateral shear is expected to dominate. Hegarty et al. (1983) noted that the thrust-faulting mechanism (P -axis oriented approximately E–W), reported by Bergman and Solomon (1980) for the 1968 event, is roughly consistent with this model. The body-waveform inversion solution for this event, however, involves a significant component of strike-slip motion. The preferred fault plane strikes NNW, parallel to the Sorol Trough and the structural grain in the epicentral area. The sense of strike-slip motion on this plane is left-lateral, which is in good agreement with the expected style of deformation in this part of the Caroline–Pacific

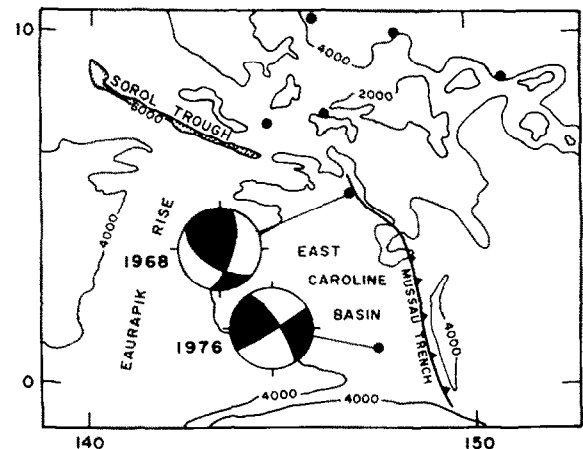


Fig. 7. Locations and focal mechanisms of the August 20, 1968 and August 30, 1976 earthquakes in the eastern Caroline Islands. Tectonic elements and bathymetry (2000 and 4000 m contours) from Nishiwaki (1981). Heavy barbed line indicates proposed site of compressional plate boundary between the Caroline and Pacific plates (Nishiwaki, 1981). Other epicenters in the region are indicated by solid circles.

boundary zone. The inferred orientation of maximum horizontal compression is nearly E–W.

The other large earthquake in the eastern Caroline Islands for which we have a source mechanism, on August 30, 1976, appears to be unrelated to any of the zones of deformation outlining the proposed Caroline plate (Fig. 7). The *P*-axis is oriented approximately NE–SW, in reasonable agreement with the relative motion between the Pacific–Caroline plate and the Indo-Australian plate at the New Guinea Trench to the southwest (Nishiwaki, 1981). There is little evidence on which to base a selection of one of the nodal planes as the fault plane.

South Fiji Basin

The May 21, 1972 earthquake and the much larger event on October 17, 1977 are located in the South Fiji marginal basin (Fig. 8). According to the tectonic history proposed for this region by Watts et al. (1977), the 1977 event is close to the boundary between oceanic lithosphere created at a system of three spreading ridges (active between 35 and 28 m.y.B.P.) and a relict subduction zone trending roughly NW–SE between New Caledonia and Northland, New Zealand. The extinct RRR triple junction is located at 26.7°S and 174.5°E, a short distance northwest of the epicenter of the May 1972 earthquake (Fig. 9). This event appears to be located precisely on the southeast-trending relict spreading center.

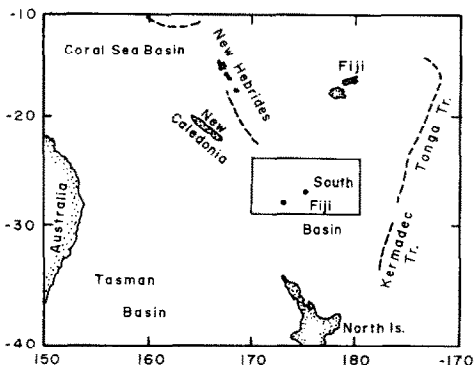


Fig. 8. Location map for the South Fiji Basin and surrounding features. The box outlines the region shown in greater detail in Fig. 9. The two dots indicate the epicenters of the May 21, 1972 and October 17, 1977 earthquakes.

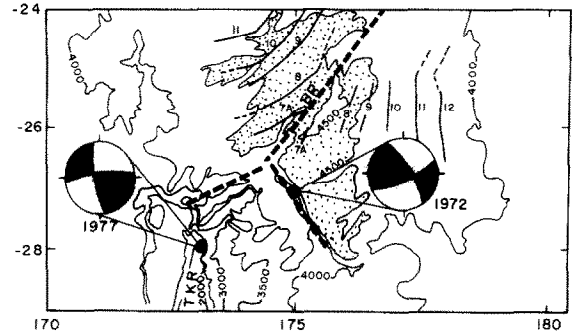


Fig. 9. Locations and focal mechanisms of the May 21, 1972 and October 17, 1977 earthquakes in the South Fiji Basin. Selected isobaths (2000–4500 m, with 500 m contour interval) and numbered magnetic anomalies are from fig. 6 of Watts et al. (1977). Region with depth > 4500 m is stippled. BR—Bounty Ridge, TKR—Three Kings Rise.

The focal mechanism of the 1972 event is characterized by right-lateral strike-slip motion on a nodal plane which is very nearly parallel with the relict spreading center, and I take this as the likely fault plane. For the 1977 event, the nodal plane striking approximately N5°W is perhaps more likely to correspond to the fault plane, because of its similarity to the inferred fault plane of the 1972 earthquake. An argument could also be made that the fault plane trends E–W, however, if the morphology of the northern end of the Three Kings Rise were attributed to its truncation by an E–W trending fracture zone. The origin of the Three Kings Rise is unclear, but Watts et al. (1977) do not associate it with the extinct spreading ridge system.

Assuming that these two earthquakes occurred on faults which are optimally oriented with respect to the existing stress field, I infer that the state of stress in the South Fiji Basin is characterized by a maximum horizontal compressive stress oriented approximately NNE. The minimum principal stress is subhorizontal and oriented ESE.

Hawaii

The source of the stress relieved in the April 26, 1973 Hilo earthquake is of particular interest, because this event, at a depth of 45 km, is one of

the deepest large oceanic intraplate earthquakes known. Smaller earthquakes have been located at depths of up to 60 km beneath the summits of the two presently active volcanoes on Hawaii, Mauna Loa and Kilauea, but the deepest such events are thought to be related to the migration of magma (e.g., Eaton, 1962; Koyanagi et al., 1972). Small mantle-depth earthquakes also occur rather uniformly beneath the entire island; it has been suggested that such events result from bending stresses in the lithosphere beneath the island load (Rogers and Endo, 1977), but too few reliable focal mechanisms are known to evaluate this hypothesis.

The orientation of principal stresses inferred from this earthquake can be compared with the

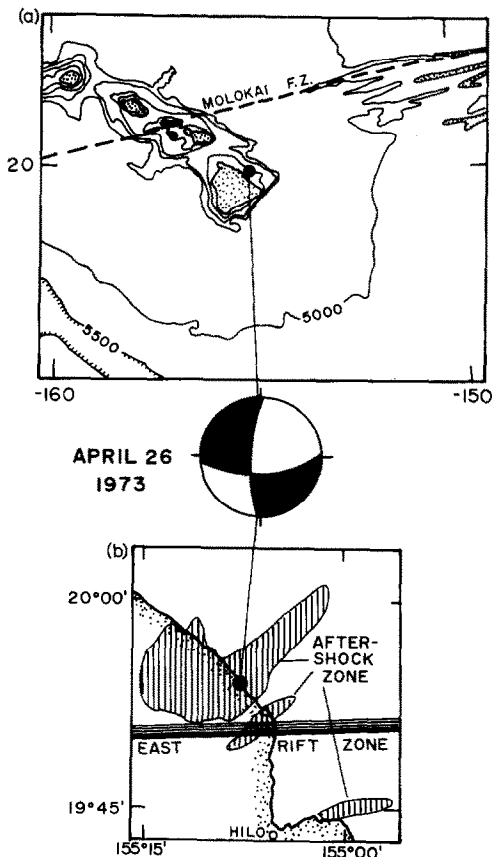


Fig. 10. Location and focal mechanism of the April 26, 1973 earthquake beneath the northeast coast of Hawaii. a, Regional bathymetry, from Drummond (1981); 500 m contours. The trend of the Molokai Fracture Zone is shown by the dashed line. b, Detailed map showing the surface projection of aftershock zone and the location of the East Rift Zone of the volcano Mauna Kea, adapted from fig. 1 of Butler (1982).

predictions of several models of the stress field in the central Pacific and the origin of the Hawaiian Island chain. The P -axis of the focal mechanism of this earthquake is subhorizontal and oriented at $N38^\circ E$, roughly radial to the island (Fig. 10). From the aftershock pattern and the waveform inversion study of this event (see the Appendix), the nodal plane striking $N83^\circ E$ was selected as the fault plane. Using the procedure suggested by Raleigh et al. (1972), the best estimate of the orientation of maximum horizontal compressive stress is $N51^\circ E$.

The orientation of the least horizontal compressive stress ($N39^\circ W$) inferred from the Hilo earthquake is inconsistent with the formation of the Hawaiian Island Chain as a propagating tensional fracture in the lithosphere (Green, 1971) or with the model of Jackson and Shaw (1975), in which the loci of volcanoes in the chain delineate the direction perpendicular to the least principal horizontal stress. A horizontal least principal stress striking $N39^\circ W$ is also incompatible (but less so) with the suggestion of Turcotte and Oxburgh (1973) that the Hawaiian Island Chain represents deformation of the Pacific plate caused by the latitudinal component of its motion over a non-spherical earth.

Using an analytical solution to the response of an elastic plate over an inviscid fluid to a cylindrical vertical load (Brotchie, 1971), I carried out a preliminary investigation of the possibility that plate bending stresses, induced by the island load, could be the dominant cause of the 1973 Hilo earthquake. Specifically, a large deviatoric compressive stress radial to the load would be required to account for the earthquake. Below the neutral plane near the edge of the load the radial deviatoric stress is extensional, not compressive, with a magnitude of several kilobars. A detailed quantitative model of bending stresses beneath Hawaii is complicated by controversy concerning some of the fundamental parameters of the problem (e.g., Suyenaga, 1979). It is unlikely, however, that refinements to the model used here would cause a reversal in the sign of the bending stresses at the position of the hypocenter.

Finally, we consider the possible relationship between the Hilo earthquake and the East Rift

Zone of the dormant volcano Mauna Kea (Jackson et al., 1972). The Hilo earthquake is approximately 45 km east of the central core of Mauna Kea. The epicenter is about 5 km north of the surface expression of the rift zone, to which the inferred fault plane is parallel (Fig. 10). The depth extent of the rift zone is unknown, but the seismicity associated with other volcanic rift zones on Hawaii is usually shallow, at depths of 15 km or less (Fiske and Jackson, 1972).

In summary, the cause of the 1973 Hilo earthquake is unclear. The evidence, while circumstantial, favors a dominant role for deep magmatic processes beneath Mauna Kea, although the intraplate stress field in the central Pacific may well have influenced the geometry of faulting.

South China Basin

The epicenter of the October 7, 1965 earthquake is in the southwestern end of the South China Basin, the westernmost marginal basin in

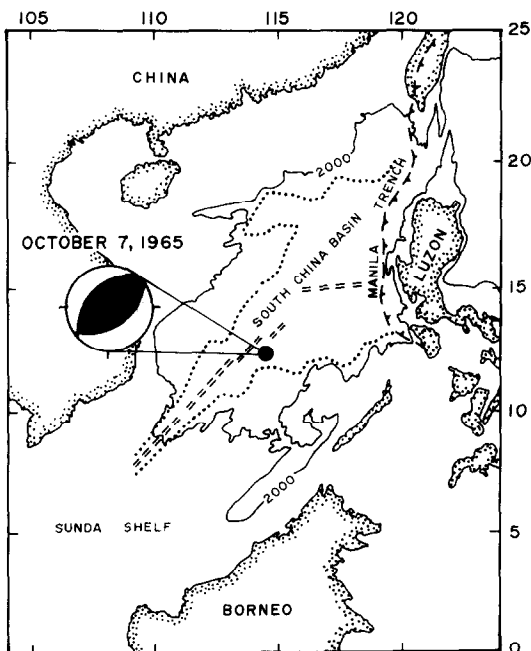


Fig. 11. Bathymetry and inferred tectonic elements in the South China Sea, together with the location and focal mechanism of the October 7, 1965 earthquake. Adapted from Fig. 17 of Taylor and Hayes (1983). The 2000 m isobath is shown. Dashed parallel lines in the southwest part of the South China Sea denote the position of a relict spreading center. Dots outline area of normal oceanic crust.

the Pacific (Fig. 11). Karig (1971) classified it as an "inactive" marginal basin. A few earthquakes have been located along the margin of the basin, but the interior has been seismically quiet (Wang et al., 1979). Most of the lithosphere in the South China Basin formed between 32 and 17 m.y.B.P. at a spreading center trending E-W. The southwestern part of the basin, however, apparently was created at a NE-trending spreading center whose axis is located only about 60 km northwest of the epicenter (Taylor and Hayes, 1983). Unfortunately, no magnetic anomalies have been identified in the area and thus there is no reliable information about the timing of this minor spreading episode. Heat flow measurements are consistent with an age similar to the rest of the South China Basin (Taylor and Hayes, 1983). The sediments in the epicentral region are relatively undisturbed, indicating that major intraplate deformation has not occurred there (Wang et al., 1979). Taylor and Hayes (1983) observed that the nodal planes of the thrust-faulting focal mechanism are subparallel to the nearby relict spreading center and suggested that it "occurred along a fault plane whose strike was largely determined by the pre-existing spreading fabric of the oceanic basement".

Philippine Sea

A small earthquake occurred on April 12, 1974 at the intersection of the extinct Central Basin

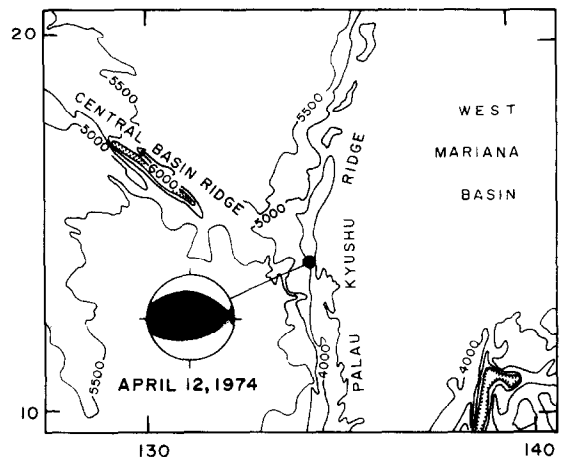


Fig. 12. Location and focal mechanism of the April 12, 1974 earthquake in the Philippine Sea. Bathymetry (500 m contour interval) from Nishiwaki (1981).

Spreading Center (CBSC) and the Palau–Kyushu Ridge, in the Philippine Sea (Fig. 12). According to Hilde and Lee (1984) the most recent episode of spreading on the CBSC (from 45 to 35 m.y.B.P.) occurred on small E–W trending ridge segments offset in a right-lateral sense by N–S trending fracture zones. The Palau Kyushu Ridge is a relict subduction zone, which may overprint a long transform fault. The mechanism of the April 1974 event is characterized by thrust faulting on nodal planes striking roughly E–W, subparallel with the strike of ridge axis segments on the CBSC.

Southeast Pacific

On February 5, 1977 a large earthquake occurred in a remote corner of the southeast Pacific, a region with a very complex tectonic history (e.g., Weissel et al., 1977; Cande et al., 1982). The lithosphere of the epicentral region was formed at the former Antarctic–Aluk spreading ridge, which along with most of the Aluk plate, has been subducted beneath the Antarctic Peninsula (Barker, 1982). The epicenter lies between two major fracture zones trending NW–SE (Fig. 13). Although an unmapped fracture zone could pass through the epicentral area, the strike of the nodal planes is oblique to the regional trend of fracture zones.

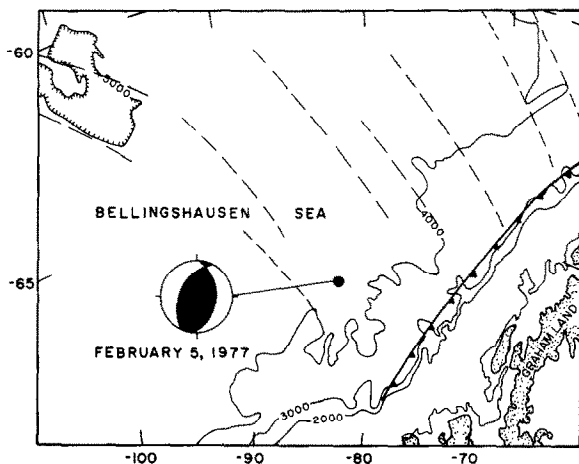


Fig. 13. Location and focal mechanism of the February 5, 1977 earthquake in the Bellingshausen Sea in the southeast Pacific. Bathymetry (1000 m contour interval) and tectonic elements from Craddock (1981). Dashed lines indicate location of fracture zones inferred from magnetic anomaly offsets. Heavy barbed line indicates location of a relict subduction zone.

The P -axis is approximately perpendicular to the Antarctic continental margin. Okal (1980) noted that the orientation of the P -axis is perpendicular to the nearest ridge system but oblique to the direction of absolute motion of the Antarctic plate, so that the earthquake is not likely to be the result of basal drag forces on the plate.

Seismic moment release as a function of age

The spatial pattern of seismic moment release is a direct reflection of the internal deformation of oceanic lithosphere and may help in identifying the dominant sources of stress resulting in seismicity. One useful way to parameterize this pattern is to consider the variation of seismic moment released in oceanic lithosphere as a function of age, since variations in the mechanical properties (e.g., Chen and Molnar, 1983; Wiens and Stein, 1983) and also in the state of stress (e.g., Dahlen, 1981) are thought to be related in fundamental ways to the age of the lithosphere.

Wiens and Stein (1983) found a marked decrease in the rate of seismic moment release with increasing lithosphere age. I perform a similar calculation here, using a catalog of 461 oceanic intraplate earthquakes for the years 1964–1979 (Bergman, 1984).

The subset of Hawaiian earthquakes (138 events) is segregated because it dominates the seismic moment release in its age category, and much of the seismic moment released there is related to volcanic rather than tectonic processes. Although the Gilbert Islands swarm of 1981–1983 (Lay and Okal, 1983) occurred outside the time window being considered, the contribution of 190 of the largest events to the seismic moment release in older oceanic lithosphere provides insight into the extent to which 16 years of intraplate seismicity can be regarded as representative of the long-term rate of internal deformation of oceanic lithosphere. The cause of this unusual burst of seismicity is open to speculation: although a tectonic origin is preferred by Lay and Okal (1983), they point out that certain characteristics of the swarm are suggestive of hot-spot magmatism.

Rather than attempt to specify a precise age for the lithosphere in which each earthquake oc-

curred, I adopted the lithospheric age categories of Slater et al. (1980) and assigned each earthquake to one of the 13 "bins" by superimposing maps of oceanic intraplate seismicity and maps of the isochrons defining the age categories. When an epicenter lies very near one of the isochrons, it has been assigned to the older age category. This was done to avoid biasing the results toward higher moment release in young lithosphere, which Wiens and Stein (1983) showed to be the dominant pattern.

A seismic moment was assigned to each earthquake, using magnitude-moment relations derived from the reported magnitudes of 58 oceanic intraplate earthquakes and the corresponding seismic moments estimated in the body waveform inversion studies:

$$\log M_0 = (2.35 \pm 0.20)m_b + (11.71 \pm 1.13)$$

$$\log M_0 = (1.12 \pm 0.07)M_S + (18.67 \pm 0.41)$$

with M_0 in dyn cm. The range given in parentheses for the regression coefficients is one standard

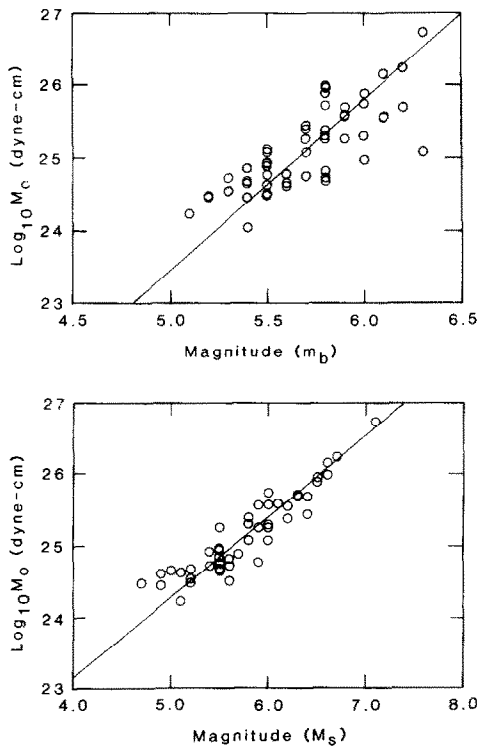


Fig. 14. Plots of m_b and M_S versus $\log_{10} M_0$ for 58 oceanic intraplate earthquakes studied with body-waveform inversion. The best fitting (in a least squares sense) lines through the data are also shown.

deviation. The data and regression lines for the two relations are shown in Fig. 14. Not surprisingly, M_0 correlates better with M_S ($r = 0.91$) than m_b ($r = 0.79$). The seismic moments of events which were not studied with the body waveform inversion were estimated from these relationships and the reported magnitude, using M_S if both magnitudes were given. If no magnitude was reported, m_b 4.5 was assumed.

The resultant seismic moment totals for oceanic intraplate earthquakes are probably underestimates for several reasons. There is no contribution from events below the threshold of teleseismic detection and location. This may be a significant factor for the moment totals in the oldest age categories, to which the western Pacific makes the largest contribution. Walker and McCreery (1985) presented evidence that global seismic networks may frequently fail to detect earthquakes with magnitudes as large as m_b 5.0 in the western Pacific. Also, the seismic moment estimated from body waves will tend to be an underestimate for the largest events studied, since the point source approximation may be invalid at the wavelengths used in the body-waveform inversion technique.

The maximum depth to which the oceanic lith-

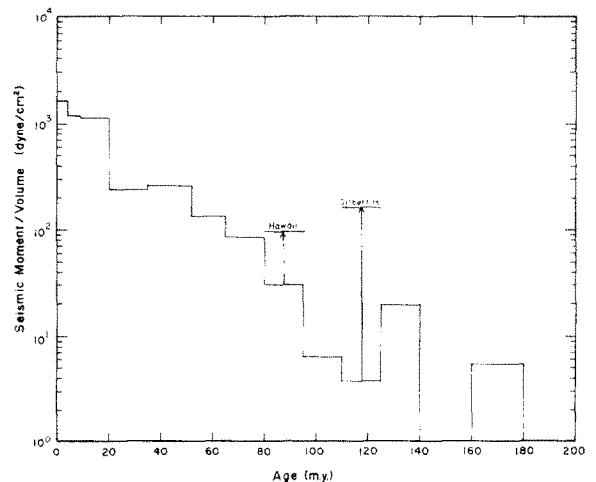


Fig. 15. Seismic moment per unit volume of lithosphere released by oceanic intraplate earthquakes as a function of age for the years 1964–1979. For the calculation of the volume of seismogenic lithosphere within each age interval, the thickness is taken equal to the average depth of the 800°C isotherm. The effect of including Hawaiian seismicity and the Gilbert Islands earthquake series of 1981–1983 are indicated. Data are listed in Table 2.

TABLE 2

Seismic moment released per unit volume as a function of lithospheric age

Age range ^a (m.y.)	Area ^a ($\times 10^6$ km ²)	Thick- ness ^b	Volume ($\times 10^8$ km ³)	Number of events	ΣM_0 ^c	M_0 /Volume (dyn/cm ²)
0- 4	14.2	7.6	1.08	23	180.0	1600.0
4- 9	19.7	14.4	2.84	66	340.0	1200.0
9- 20	31.8	21.6	6.87	98	790.0	1200.0
20- 35	42.6	29.8	12.7	104	310.0	240.0
35- 52	37.0	37.5	13.9	35	360.0	260.0
52- 65	29.7	43.6	12.9	43	170.0	130.0
65- 80	37.3	48.4	18.1	41	160.0	86.0
80- 95 ^d	27.9	53.0	14.8	18 (156)	44.0 (140.0)	30.0 (97.0)
95-110	24.8	57.0	14.1	6	8.9	6.3
110-125 ^e	15.2	60.3	9.17	8 (198)	3.4 (150.0)	3.7 (160.0)
125-140	16.7	63.1	10.5	16	21.0	20.0
140-160	8.3	65.6	5.44	1	0.10	0.18
> 160	3.4	67.8	2.31	2	1.3	5.4

^a Age ranges and corresponding areas from Sclater et al. (1981).

^b Thickness (km) calculated as the average depth to the 800°C isotherm in the age range of interest, using the cooling model of Parsons and Sclater (1977).

^c Sum of seismic moments ($\times 10^{24}$ dyn cm) of all earthquakes in the age range of interest for the period 1964-1979.

^d Values in parenthesis include Hawaiian seismicity.

^e Values in parenthesis include the Gilbert Islands seismicity of 1981-1983.

osphere is capable of accumulating strain sufficient to result in an earthquake appears to be well-approximated by the depth to an isotherm in the range of 600°C to 800°C (Chen and Molnar, 1983; Wiens and Stein, 1983, 1984; Bergman and Solomon, 1984) and thus varies strongly with age, especially in young lithosphere. Therefore, to gain a meaningful picture of the variation with age of the intensity of internal deformation of oceanic lithosphere, the seismic moment released in each age category should be normalized by the corresponding volume of seismogenic lithosphere in that age range. The depth used to calculate this volume is the average depth to the 800°C isotherm, calculated with the plate cooling model of Parsons and Sclater (1977); the area in each age category is given by Sclater et al. (1980). Data pertaining to this calculation are listed in Table 2 and the results are shown in Fig. 15.

As expected there is a strong decrease with age of the seismic moment release per unit volume of seismogenic lithosphere. A particularly large drop occurs between the 9-20 m.y. and 20-35 m.y. bins. A detailed study of the source mechanisms

of larger earthquakes in young oceanic lithosphere (Bergman and Solomon, 1984) suggests that this drop occurs at about 15 m.y. From 20 to 80 m.y., the decline in seismic moment release appears to be quite gradual. The number of earthquakes contributing to the sum of seismic moment released in oceanic lithosphere older than 80 m.y. (excluding the Hawaiian and Gilbert Islands earthquakes) is small and the calculated values of moment release per unit volume therefore have more scatter, but the general tendency for a steady decrease with age is evident.

A decrease with age of seismic moment release per unit volume of seismogenic lithosphere for ages greater than 20 m.y. is not so evident, however, if the Hawaiian and Gilbert Islands earthquakes are included in the calculation. The Gilbert Islands earthquakes are sufficient to raise the moment release per unit volume of lithosphere aged 110-125 m.y. to a value higher than that of lithosphere 52-65 m.y. old. The Gilbert Islands swarm (or the Hawaiian seismicity) is not tectonically equivalent, however, to an equal number of events (with the same cumulative moment) scatter-

ed in space and time, but assigned to the same age bin. Thus, it would be misleading to reach a conclusion about the general pattern of seismic moment release in oceanic lithosphere without distinguishing the special nature of the Gilbert Islands swarm. Nevertheless, this example raises the possibility that a large fraction of intraplate deformation may occur as intensive bursts of activity at very long intervals; the widely scattered small events which characterize many oceanic regions may simply be background noise in between such bursts.

Although many more events contribute to the estimated seismic moment release in younger lithosphere and these values are more stable than those for older lithosphere, a single large event may still cause large fluctuations. On November 30, 1983 the largest oceanic intraplate event in recent decades ($M_s = 7.5$) occurred near the Chagos Bank in the Indian Ocean, in lithosphere about 35 m.y. old. This earthquake, with a seismic moment exceeding 10^{27} dyn cm (Wiens and Stein, 1984), would completely dominate the calculation of seismic moment release per unit volume in any age range to which it might be assigned. The Chagos Bank region has been quite active since the early 1900's (Wiens, 1986), especially so over the last several decades, and may be more closely related to the exceptionally complex intraplate tectonics of the northern Indian Ocean than to a global pattern of intraplate activity (Wiens et al., 1985).

Centroid depth–age relations

The relationship between the depth of oceanic intraplate seismicity and lithospheric age is an important source of information on the evolution of the thermal and physical state of oceanic lithosphere. It also provides constraints on the relative importance of various sources of stress in the lithosphere, particularly when the source mechanisms of intraplate earthquakes are considered. Chen and Molnar (1983) and Wiens and Stein (1983) have previously studied age–depth relations for oceanic intraplate earthquakes in all ages of lithosphere, but the data set used here is more extensive, particularly for younger lithosphere. The

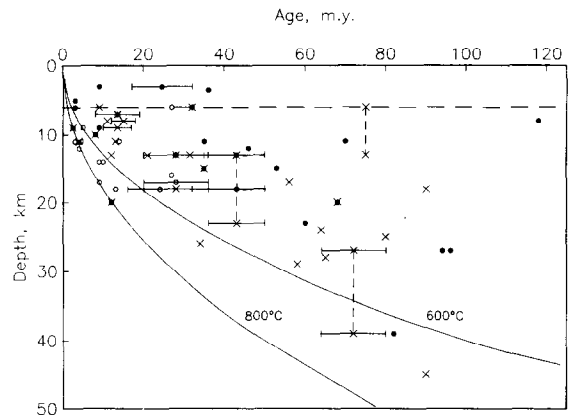


Fig. 16. Centroid depth versus lithosphere age for 58 oceanic intraplate earthquakes studied with the body-waveform inversion technique. The earthquakes are distinguished on the basis of fault type. Symbols are: open circle—normal, solid circle—thrust, \times —strike-slip. Two symbols are superimposed where the mechanism is intermediate in type. Depths are relative to the seafloor. The horizontal dashed line indicates the depth of the Moho (6 km) in the velocity model used for the inversions, but the velocity model used for some events in older lithosphere also has a sediment layer (see individual source studies). Error bars are given for some events (usually those located on fracture zones with significant offset) for which there is significant uncertainty in the appropriate lithosphere age. Uncertainty in the centroid depths is typically about 2 km. For three earthquakes (October 10, 1970, April 7, 1973, and June 25, 1974) which were modelled as multiple events by Bergman and Solomon (1985), the centroid depths of the subevents are plotted separately and connected by vertical dashed lines. The 600° and 800°C isotherms, calculated from the plate-cooling model of Parsons and Sclater (1977), are also shown.

variations with depth and lithosphere age of the source parameters of earthquakes in young oceanic lithosphere have been thoroughly discussed by Bergman and Solomon (1984) and Wiens and Stein (1984).

The centroid depths of 58 oceanic intraplate earthquakes are plotted against the age of the lithosphere in Fig. 16. The source studies of those events not presented here are reported in Bergman and Solomon (1984, 1985). The faulting style of each event is indicated. The 600° and 800°C isotherms calculated with the cooling plate model of Parsons and Sclater (1977) are also shown.

Previous studies of the variation of the maximum depth of oceanic intraplate seismicity with lithospheric age suggest that the maximum depth at a given age is limited by the depth to an

isotherm in the range 600° to 800°C (Chen and Molnar, 1983; Wiens and Stein, 1983). The data in Fig. 16 are consistent with this conclusion, but the additional data for earthquakes in young oceanic lithosphere reveal a possible discontinuity in the limiting isotherm at about 12 m.y. In younger lithosphere, the maximum depth of seismicity corresponds to temperatures near 800°C, while the limiting isotherm in older oceanic lithosphere is closer to 600°C.

The convergence of isotherms at young ages and the uncertainty in centroid depth, typically about 2 km, leads to considerable uncertainty in assigning a corresponding limiting temperature to any individual earthquake in young lithosphere. There are seven events whose centroid depths place them near the 800° isotherm in Fig. 16. Random errors cannot account for this many such observations and the possibility of a significant systematic bias has been effectively eliminated by numerous tests and intercomparisons with the results of other researchers, using different data and methods. It should also be noted that the centroid depth represents an average over the entire region of faulting. The maximum depth extent of faulting almost certainly extends several kilometers deeper. Therefore 800° is a rather conservative estimate of the isotherm limiting the depth of faulting in young oceanic lithosphere.

This discontinuity in the isotherm controlling the maximum depth of faulting suggests that the deepest events in young lithosphere may release stresses originating from a physical process different from that which controls the deepest seismicity in older lithosphere. This hypothesis is supported by the observation that all the events in young lithosphere whose centroid depths approach or exceed the depth of the 800°C isotherm are characterized by a large component of normal faulting, whereas the deepest events in older lithosphere are all characterized by strike-slip or thrust faulting. Bratt et al. (1985) demonstrated that thermoelastic stresses arising during the rapid early cooling of the oceanic lithosphere (and possibly intensified by thermal perturbations associated with small-scale convection near the lithosphere–asthenosphere boundary) are a likely cause of deep normal-faulting earthquakes in young oc-

eanic lithosphere. Bergman and Solomon (1984) argued that the deepest normal-faulting earthquakes in young oceanic lithosphere may be associated with average strain rates as high as 10^{-13} s^{-1} .

Bergman and Solomon (1984) noted that thrust faulting in young oceanic lithosphere seems to be confined to depths shallower than about 10 km below the seafloor. Figure 16 shows that thrust faulting occurs throughout the seismically-active depth interval in lithosphere older than about 30 m.y., but most of these events are found in the northern Indian Ocean, where the entire elastic core of the lithosphere may be subject to an unusually large horizontal compressive stress (Bergman and Solomon, 1985). The only other earthquake in old oceanic lithosphere with a significant component of thrust faulting and a centroid deeper than 20 km (December 13, 1977) is associated with the diffuse boundary between the North and South American plates. With these exceptions, thrust faulting is observed only at relatively shallow depths, and very seldom in lithosphere older than about 50 m.y.

Discussion

In this section, I present a synthesis of the global distribution of oceanic intraplate seismicity, the rate of seismic moment release as a function of age, the source mechanisms and tectonic associations of larger events, and the depth-dependence of various source parameters to address several aspects of the relationship between earthquakes and the intraplate stress field in oceanic lithosphere. First I consider the reliability of stress orientations inferred from earthquake source mechanisms. The differences between seismicity in young and old oceanic lithosphere and the relative aseismicity of old oceanic lithosphere in the western Pacific are discussed. Finally, the extent to which oceanic intraplate earthquakes may be useful in investigating plate driving forces is considered.

Earthquakes as indicators of the state of stress

Uncertainty concerning the use of focal mechanisms to infer the state of stress in the lithosphere

arises from two sources, uncertainty in the focal mechanism itself and theoretical problems with the relationship between the principal axes of the focal mechanism and the pre-earthquake state of stress in the volume of lithosphere encompassing the earthquake source (McKenzie, 1969).

The now-common use of waveform modeling for body wave phases yields a significant improvement over first-motion studies in resolving focal mechanisms. With good station coverage and the use of both P and SH waveform data, uncertainty in the focal mechanism is essentially removed as a source of error in inferring the state of stress in the epicentral region. A further advantage to waveform modeling results when the fault plane can be determined from horizontal directivity in the rupture, allowing a refined estimate of the principal stress directions to be made (Raleigh et al., 1972).

Observational evidence indicates that focal mechanisms are a generally reliable indicator of stress. The Rangely, Colorado, experiment in induced seismicity (Raleigh et al., 1972) is an excellent example. Zoback and Zoback (1980), in their study of the state of stress throughout the conterminous United States, found good agreement between stress orientations derived from a variety of indicators, including focal mechanisms, young

geological features, and direct stress measurements.

From the realm of oceanic intraplate studies, the consistency of stress orientations inferred from focal mechanisms (with varying faulting styles) in the northern Indian Ocean (Bergman and Solomon, 1985), between the lesser Antilles and the Mid-Atlantic Ridge, in the South Fiji Basin, from the Gilbert Islands earthquake series (Lay and Okal, 1983) and earthquakes in the south-central Pacific (Okal et al., 1980) support the contention that focal mechanisms are generally reliable indicators of the state of stress in the source region. Finally, an in situ stress measurement in the upper oceanic crust at DSDP hole 504B in the northeastern Nazca plate (Newmark et al., 1984) is in good agreement with the directions of principal stresses inferred from focal mechanisms of several intraplate earthquakes in the region, even some on the opposite side of the Cocos–Nazca spreading center (Fig. 17).

That earthquake focal mechanisms are empirically rather reliable indicators of stress is probably a reflection of the fact that an earthquake will occur most readily on a fault plane oriented such that the resolved shear stress is maximized while the normal stress across the fault and thus the frictional resistance to faulting is minimized. The scale of heterogeneity relevant to earthquakes of moderate size is perhaps several tens of kilometers. At the dominant wavelength of the intraplate stress field (hundreds to thousands of kilometers), oceanic lithosphere in most regions contains such heterogeneities in virtually every orientation. Thus, intraplate earthquakes tend to occur on faults oriented favorably with respect to the ambient stress field, and their focal mechanisms are therefore relatively reliable indicators of the orientations of the principal stress axes (particularly if the fault plane can be identified).

Earthquakes in young oceanic lithosphere

Both in terms of number of events and seismic moment release, oceanic lithosphere less than about 35 m.y. old is far more active than older lithosphere (Fig. 15). Normal-faulting earthquakes are observed rather frequently in young litho-

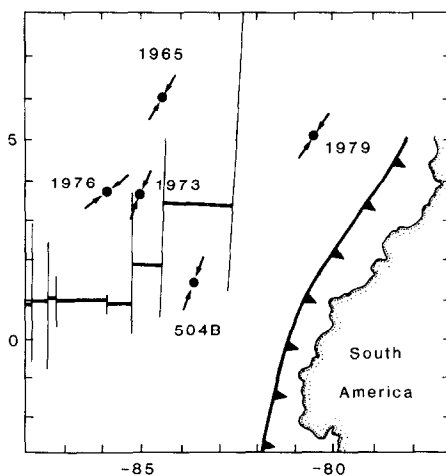


Fig. 17. Orientation of maximum horizontal compression inferred from an in-situ stress measurement at DSDP hole 504B compared with the orientations inferred from focal mechanisms of several oceanic intraplate earthquakes in the eastern Pacific. Adapted from fig. 5 of Newmark et al. (1984).

sphere, but are absent in older lithosphere (Fig. 16). The limiting isotherm for depth of faulting is higher in young lithosphere, suggesting higher average strain rates. These and other characteristics of earthquakes in young oceanic lithosphere may be largely explained if thermoelastic stresses related to the rapid early cooling of oceanic lithosphere are the dominant component of the stress field (Bratt et al., 1985).

It should be noted that the catalog of earthquakes in young oceanic lithosphere is dominated by events in the Indian plate. In favoring stresses related to the early evolution of oceanic lithosphere (thermoelastic stresses in particular) as the dominant cause of such seismicity, I assume that the Indian Ocean is distinctive in the level of activity, but not in the basic physical processes leading to seismic failure. An important test of this assumption will be the extent to which future seismicity along other plate boundaries follows the pattern in Fig. 16.

Compressive stresses due to elevated topography at the ridge axis (e.g., Dahlen, 1981) and stresses related to other forces on the plates are undoubtedly present in young oceanic lithosphere as well, but they are almost certainly small in comparison to the kilobar levels easily reached by thermoelastic stresses (Bratt et al., 1985). Since thermoelastic stresses and other stresses associated with the early evolution of oceanic lithosphere can give rise to a wide range of faulting styles, it will be quite difficult to extract information concerning the forces driving plate motions from earthquakes in lithosphere less than about 35 m.y. old.

Earthquakes in old oceanic lithosphere

In lithosphere older than about 35 m.y., virtually all the larger oceanic intraplate earthquakes have centroid depths in excess of about 12 km (Fig. 16). Because of the rapid increase of strength with depth in the upper few tens of kilometers of the oceanic lithosphere, these earthquakes are more likely than shallow events to have released stresses associated with the long-wavelength tectonic stress field. The brittle strength of the oceanic crust and uppermost oceanic mantle is probably too low for

significant stresses to be transmitted very far from their source. The March 1978 Bermuda rise event and the earthquake in November 1974 near the South Sandwich Arc are examples of relatively shallow events in old lithosphere which are probably related to local sources of stress. The Hawaiian event on April 26, 1973 is the deepest large oceanic intraplate event, but it is probably dominated by local tectonics as well.

Several of the remaining earthquakes in old lithosphere of the Atlantic Ocean are associated with a diffuse plate boundary zone between the North and South American plates. Intraplate seismicity in the northern Indian Ocean, which accounts for a large fraction of the activity in older oceanic lithosphere, is strongly influenced by the continental collision between India and Eurasia (Bergman and Solomon, 1985), and Wiens et al. (1985) have suggested that much of the seismicity may be related to a diffuse plate boundary. Lithospheric stresses in this area are probably both unusually large and spatially variable (Cloetingh and Wortel, 1985).

Most of the large intraplate earthquakes in the Pacific are associated either with marginal basins and relatively youthful lithosphere or an incipient plate boundary. Only the February 5, 1977 earthquake in the southeastern Pacific appears to be a true intraplate event in old oceanic lithosphere. Compared with the Atlantic Ocean, the Cretaceous lithosphere of the western Pacific is notably lacking in larger intraplate earthquakes, even when pre-WWSSN seismicity is included (Okal, 1984). The scarcity of smaller ($m_b < 5.5$) events can be attributed, at least in part, to detection thresholds (Walker and McCreery, 1985).

Okal (1984) proposed that the aseismicity of older oceanic lithosphere in the Pacific is the result of the reorganization of plate boundaries in the eastern Pacific in the Miocene, which left the major fracture zones in the western Pacific favorably oriented to relieve "ridge push" stresses so that the stress necessary for a large (magnitude 6) earthquake seldom accumulates.

There is little evidence that isolated intraplate earthquakes occur preferentially on large fracture zones. The March 1978 Bermuda event provides clear support for this view, since its location is

known with unusual accuracy and fracture zones in the epicentral area are well-mapped and oriented close to the strike of the nodal planes of the thrust-faulting mechanism (Nishenko and Kafka, 1982). If one looks closely enough, it is usually possible to identify a "zone of weakness" of some sort on which an earthquake occurred, but it does not follow that larger features are more prone to failure. Studies of gravity and bathymetry across large Pacific fracture zones indicate that the lithosphere "heals" quite soon after leaving the active transform and can support indefinitely bending stresses of the order of a kilobar (Sandwell and Schubert, 1982), significantly higher than the stress due to "ridge push" (e.g., Dahlen, 1981). Large-scale heterogeneities in oceanic lithosphere are perhaps prone to reactivation by thermal perturbations or the evolution of plate driving forces, with attendant concentration of intraplate seismicity, to the extent that some such zones may be better described as diffuse, incipient, or reactivated plate boundaries, but the heterogeneities in lithospheric strength which are most relevant to individual earthquakes have significantly shorter length scales. Over areas with dimensions equivalent to the dominant wavelengths of the lithospheric stress field, such heterogeneities occur in virtually every orientation.

For these reasons, I attribute the relative aseismicity of the western Pacific basin, and the general decline in seismicity in old oceanic lithosphere, to the increase in strength of the lithosphere as it cools and thickens, combined with a low ambient stress field. After perhaps 20 m.y., the cooling of oceanic lithosphere proceeds too slowly to generate thermoelastic stresses of significant magnitude (Bratt et al., 1985) and the state of stress in a large expanse of old oceanic lithosphere such as the western Pacific is likely to be dominated by the distributed "ridge push" force (Richardson et al., 1979; Richardson, 1983). The magnitude of this stress increases with age as $t^{1/2}$, approaching several hundred bars in old ocean basins (Dahlen, 1981). Old stable oceanic lithosphere is easily capable of supporting such stresses.

Intraplate earthquakes and plate driving forces

As I have discussed above, it is probably impossible to extract information about plate driving forces from earthquakes in young oceanic lithosphere, because of the dominance of stresses (predominantly thermal) related to the early evolution of the lithosphere. In old oceanic lithosphere, the stresses inferred from large earthquakes generally reflect the regional tectonic stress field, which is dominated in most cases by plate driving forces. Over large expanses of old, stable oceanic lithosphere, however, the ambient level of stress due to plate driving forces is too low to result in large earthquakes. With few exceptions, large earthquakes occur only where the level of stress is anomalously high or where the lithosphere is substantially weakened. Therefore, the number of sites in old oceanic lithosphere at which we can expect to be able to infer the orientation of the intraplate stress field is rather limited.

Many of the small ($m_b < 5.4$) earthquakes which are more evenly distributed throughout the older portions of the ocean basins (Fig. 1) may represent the influence of the distributed "ridge push" force. The stress is largest at the seafloor, negligible in young lithosphere, and increases very slowly in old lithosphere (Dahlen, 1981). Therefore, related seismicity is probably most common in lithosphere of intermediate age (where the stress first approaches the maximum value it will attain) and at shallow depths. To the extent that other stresses in oceanic plates, such as the net force at a subduction zone, are applied and transmitted through the strong core of the lithosphere, they are probably seismically expressed primarily in the large deep events discussed above. Richardson and Cox (1984) found the area-integrated "ridge push" stress field associated with the actual topography of the Nazca plate to be quite complicated, however. This factor, coupled with the extreme difficulty in determining focal mechanisms of small remote earthquakes, severely complicates a general investigation of the oceanic intraplate stress field in this manner, although analysis of smaller events could prove fruitful in special circumstances.

Conclusions

Large oceanic intraplate earthquakes are frequently associated with disturbed regions of the oceanic lithosphere, such as fracture zones, relict spreading centers, and lithosphere created during episodes of reorientation of spreading centers. Because the heterogeneities which may act to localize seismic failure are found in many orientations throughout most ocean basins, oceanic intraplate earthquakes are nonetheless generally reliable indicators of the stress field in the source region.

The maximum observed depth of oceanic intraplate seismicity at any age appears to be limited by an isotherm, but the isotherm appropriate to earthquakes in lithosphere less than about 20 m.y. old appears to be 150–200° higher than that for older lithosphere: 800° and 600°C, respectively, when isotherms are calculated with the cooling plate model of Parsons and Sclater (1977). Under the assumption that the mechanism of rupture is invariant, the most likely cause of this observation is a higher characteristic strain rate associated with the deepest events in younger lithosphere.

A large proportion of oceanic intraplate seismicity occurs in lithosphere younger than about 35 m.y. old. Much of this seismicity is probably dominated by stresses related to the early thermal evolution of the lithosphere. Thermoelastic stresses in young oceanic lithosphere may arise rapidly enough to account for the presumed high strain rate which would account for the relatively high limiting isotherm noted above. The contribution to the tectonic stress field of plate driving forces is relatively minor in young oceanic lithosphere and cannot be recovered reliably from earthquake source studies.

In oceanic lithosphere older than perhaps 60 m.y., where the intraplate stress field is dominated by the distributed ridge-push force and possibly other plate driving forces of comparable magnitude, the lithosphere has cooled, thickened, and stabilized to the extent that seismic failure occurs rarely. All earthquakes in lithosphere older than 35 m.y. are characterized by thrust or strike-slip faulting, indicating an intraplate stress field dominated by horizontal compression. Most earthquakes in older lithosphere have depths 10

km or more below the seafloor, where the increasing strength of the lithosphere allows stresses to be transmitted significant distances across the plate. Large earthquakes in old oceanic lithosphere are not randomly distributed throughout the oceans, however, but are commonly associated with a small number of zones of major intraplate deformation or diffuse plate boundaries, where the lithosphere has been substantially weakened or stresses are anomalously high. The regional state of stress is accurately reflected in the focal mechanisms of large intraplate events, but the number of such regions is limited.

APPENDIX

Source mechanisms from long-period body-wave-form inversions

I present here details of the source studies, by inversion of teleseismic P and SH waveforms, of 15 intraplate earthquakes in the Atlantic and Pacific Oceans. The source parameters are summarized in Table 1. The inversion procedure follows the method of Nabelek (1984), and is described by Bergman et al. (1984) and Bergman and Solomon (1984). Except where noted, all inversions were performed with the same source velocity structure: a water layer with depth estimated from bathymetric maps, a single crustal layer of thickness 6 km, seismic velocities $\alpha = 6.4$ km/s and $\beta = 3.7$ km/s, and density $\rho = 2.9$ g/cm³, and a mantle halfspace with $\alpha = 8.1$ km/s, $\beta = 4.6$ km/s, and $\rho = 3.4$ g/cm³. A sedimentary layer was included in some cases. Focal depths are given relative to the seafloor. The convention for describing a double-couple source mechanism is that of Aki and Richards (1980): the strike and dip of one nodal plane are given and the slip angle defines the motion of the hanging wall relative to the footwall, measured counterclockwise from strike on the foot wall. The three angles are given in the order: strike/dip/slip.

The earthquakes are discussed in chronological order. Following the date of each earthquake, the figure numbers for the map of the epicentral region and for the comparison of synthetic and observed seismograms are given in parentheses.

The station codes and locations of seismograph stations used for the body-waveform inversions are given by Poppe et al. (1978).

October 23, 1964 (Figs. 5 and A1)

Molnar and Sykes (1969) examined first motion data from the October 23, 1964 event in the western Atlantic and determined a strike-slip mechanism (with a small component of thrusting): 284/52/137. Fitch (1981) inverted P waveforms and found a mechanism similar to that of Molnar and Sykes, but with a larger strike-slip component. He also reported a centroid depth of 23 km and a seismic moment of 8.1×10^{25} dyn cm. Liu and Kanamori (1980) modeled P waveforms in the forward sense, finding a focal mechanism of 296/66/158, a seismic moment of 6.2×10^{25} dyn cm and a depth of 23 km. Stein et al. (1982) also

modeled the P waveforms; their preferred focal mechanism (302/62/160) is similar to the other estimates, but their estimate of the seismic moment (4.5×10^{25} dyn cm) is somewhat smaller and their depth of 30 km is somewhat larger than the others.

The distribution and quality of P waveform data for the inversion is quite good, but only 6 usable SH waves were obtained. The best fitting focal mechanism is similar to those discussed above (285/56/152), except that it is rotated about 15° counterclockwise from that of Stein et al. (1982). The seismic moment is 5.2×10^{25} dyn cm, in good agreement with the estimates of Liu and Kanamori and Stein et al. The centroid depth of 28 km is slightly shallower than that of Stein et al. (1982). Both Liu and Kanamori (1980) and Fitch (1981) used halfspace source structures with crustal velocities and thus underestimated the depth of

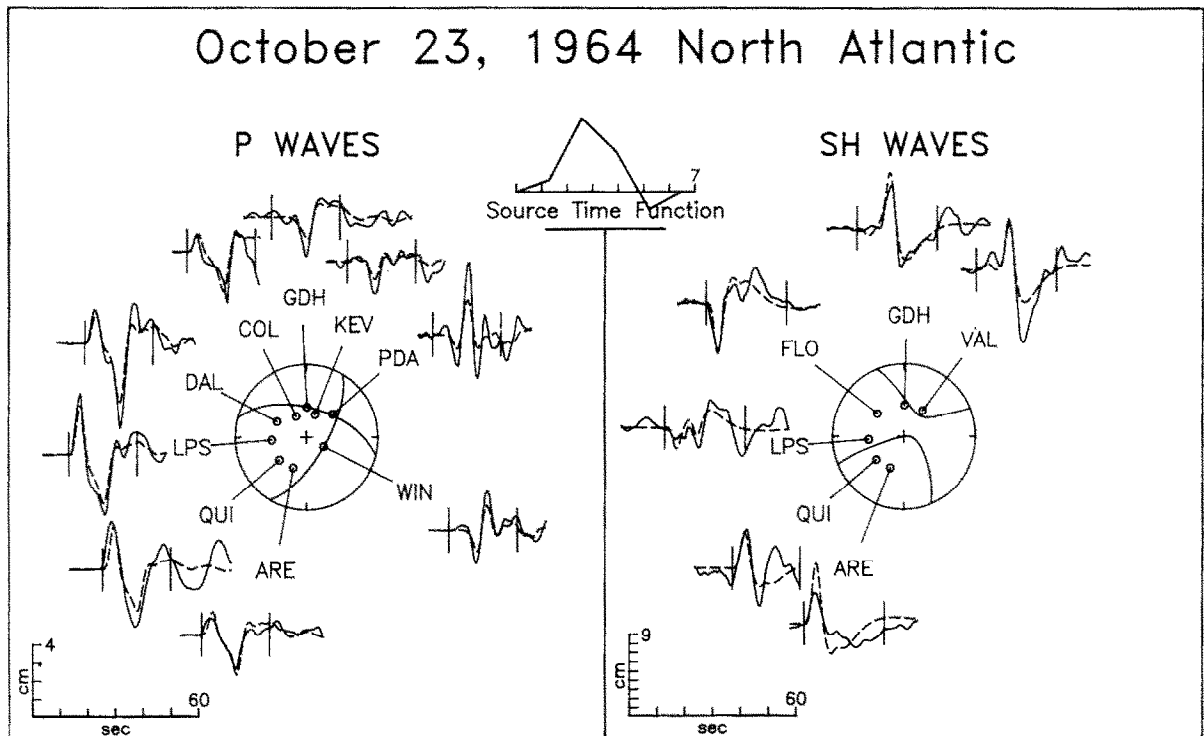


Fig. A1. Comparison of observed (solid line) long-period P and SH waves from the October 23, 1964 earthquake with synthetic waveforms (dashed lines) generated for the best-fitting point source mechanism found in the body-waveform inversion. P and SH radiation patterns are shown on the lower focal hemisphere (equal area projection). All amplitudes are normalized to an instrument magnification of 3000; the amplitude scales correspond to the waveforms that would be observed on an original seismogram from such an instrument. The two vertical lines delimit the portion of each time series used in the inversion. For SH waves, compression corresponds to positive motion as defined by Aki and Richards (1980).

the earthquake. The depth estimate is controlled primarily by the P waveforms at stations to the west and southwest (ARE, QUI, LPS, DAL, and COL). The other P waveforms are near-nodal and therefore contain little depth information.

October 7, 1965 (Figs. 11 and A2)

Using surface wave radiation patterns, Wang et al. (1979) determined a thrust-faulting mechanism for the October 7, 1965 event in the South China Basin (240/50/100) and a seismic moment of 1×10^{25} dyn cm. They also modeled P waveforms to constrain the depth to be very shallow, about 5 km below the seafloor. From the body waves, they estimated a seismic moment of 9×10^{24} dyn cm. The inversion solution is similar, but rotated counterclockwise about 20° (218/43/83) from that of Wang et al. The centroid depth is 3 km and the moment is 5.5×10^{24} dyn cm, significantly smaller than the estimate of Wang et al. The P waveforms are well-matched in shape and am-

plitude by this solution. The SH waves from this earthquake are relatively small and the signal-to-noise ratio is poor; as a result, the resolution of the strike and slip angles of the double couple mechanism is reduced.

August 20, 1968 (Figs. 7 and A3)

Using first motion polarities, Bergman and Solomon (1980) obtained a thrust-faulting mechanism (160/43/60) for the August 20, 1968 earthquake in the western Pacific. The slip angle is constrained only by the polarity of several near-nodal arrivals. Using this mechanism, Wiens and Stein (1983) modeled P waveforms and estimated the depth to be 10 km below the seafloor. The body-waveform inversion indicates that this earthquake has a larger component of strike-slip motion than the mechanism of Bergman and Solomon: 126/54/35. The distribution of stations for this event is quite poor. The centroid depth is

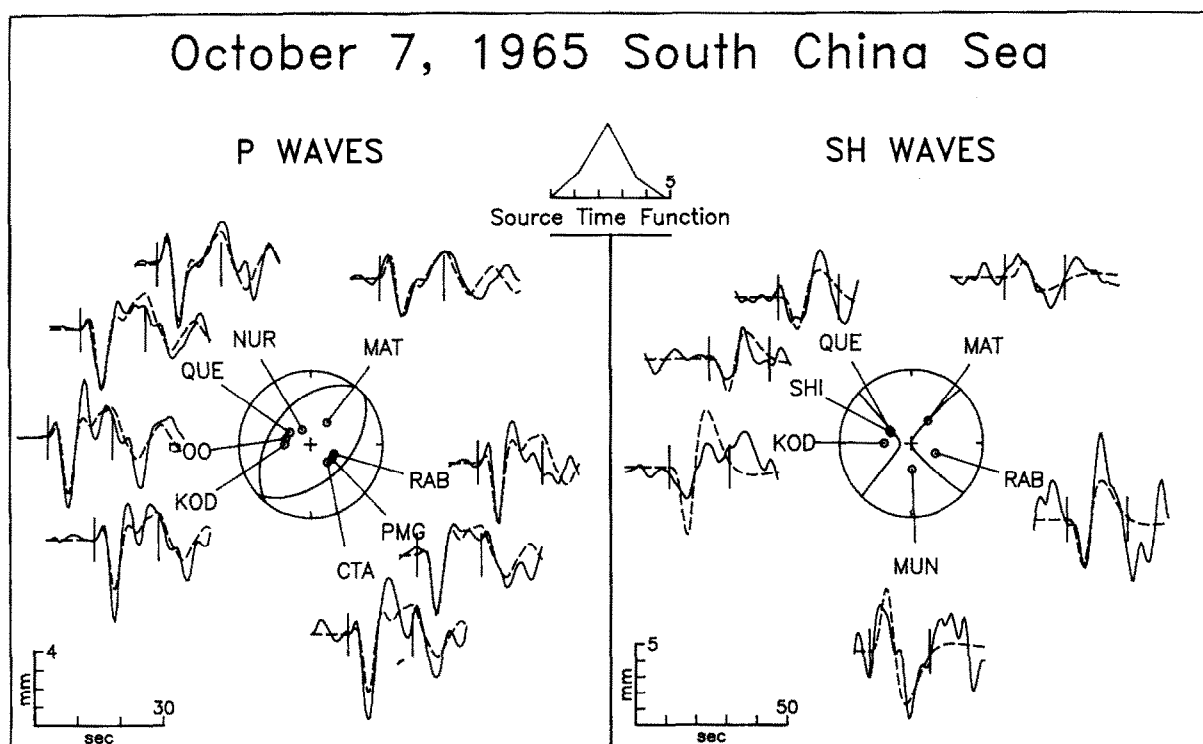


Fig. A2. Comparison of observed (solid line) long-period P and SH waves from the October 7, 1965 earthquake with synthetic waveforms (dashed lines) generated for the best-fitting point source mechanism found in the body-waveform inversion. See Fig. A1 for further explanation.

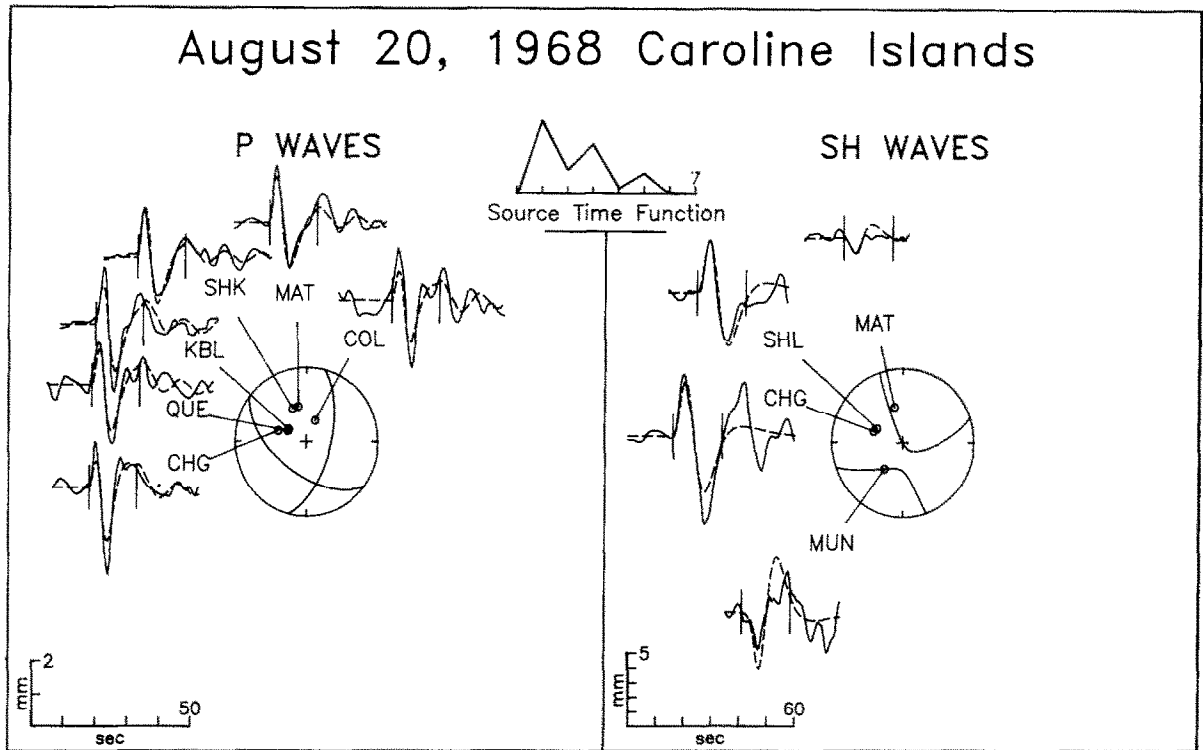


Fig. A3. Comparison of observed P and SH waves from the August 20, 1968 earthquake with synthetic waveforms generated for the best-fitting point source mechanism found in the body-waveform inversion. See Fig. A1 for further explanation.

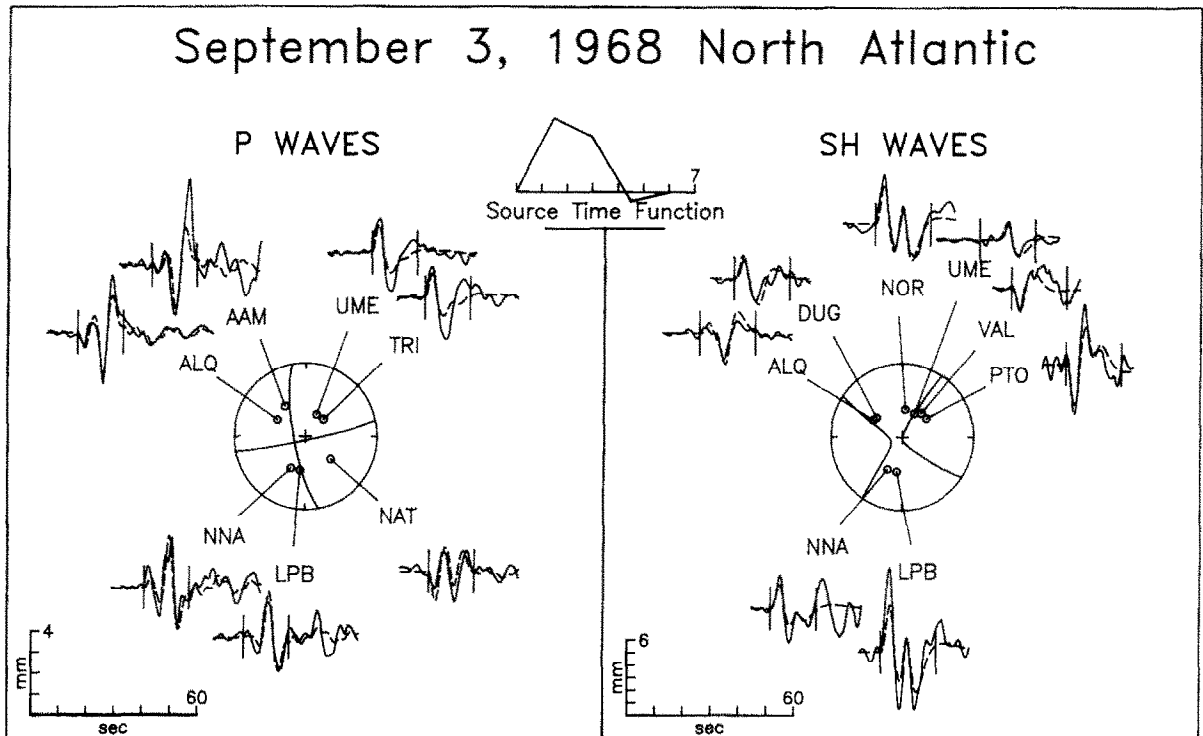


Fig. A4. Comparison of observed P and SH waves from the September 3, 1968 earthquake with synthetic waveforms generated for the best-fitting point source mechanism found in the body-waveform inversion. See Fig. A1 for further explanation.

6 km and the seismic moment is 5.3×10^{24} dyn cm.

September 3, 1968 (Figs. 5 and A4)

Sykes and Sbar (1974) reported a thrust-faulting first-motion solution (209/55/95) for the September 3, 1968 event in the western Atlantic, but Wiens and Stein (1983) found that the P waveforms required a strike-slip mechanism (176/76/0). The body-waveform inversion converged to a mechanism quite similar to that of Wiens and Stein: 168/76/4. The station distribution for both P and SH waves is good. Both nodal planes of the SH wave radiation pattern are well constrained by stations with nodal direct phases (UME and ALQ). The centroid depth of this event is 25 km, close to the depth of 27 km reported by Wiens and Stein (1983). The seismic moment is 6.6×10^{24} dyn cm.

September 30, 1971 (Figs. 2 and A5)

Sykes and Sbar (1974) reported a predominantly thrust-faulting mechanism (72/60/117) for

the September 30, 1971 earthquake in the equatorial Atlantic, based on P wave first motions and shear wave polarizations. Liu and Kanamori (1980) studied the source mechanism by modeling P and SH waveforms, preferring a mechanism with a larger (and in the opposite sense) component of strike-slip motion (72/60/60). Liu and Kanamori found a best-fitting depth of 13 km below the top of a halfspace with crustal velocities and a seismic moment of 7×10^{24} dyn cm. Their source time function is a symmetric trapezoid with a total length of 1.6 s.

The source velocity structure used for the inversion includes a sediment layer 1.5 km thick, with $\alpha = 2.0$ km/s, $\beta = 0.9$ km/s, and $\rho = 2.3$ g/cm³ (Sibuet and Mascle, 1978). The station distribution is excellent and a very good fit to the observed waveforms was obtained with a mechanism similar to that of Liu and Kanamori, but with a larger component of thrust faulting (79/60/74). The centroid depth is 12 km below the top of the sediment layer. The seismic moment is 1.1×10^{25} dyn cm. The first pulse of the source time function

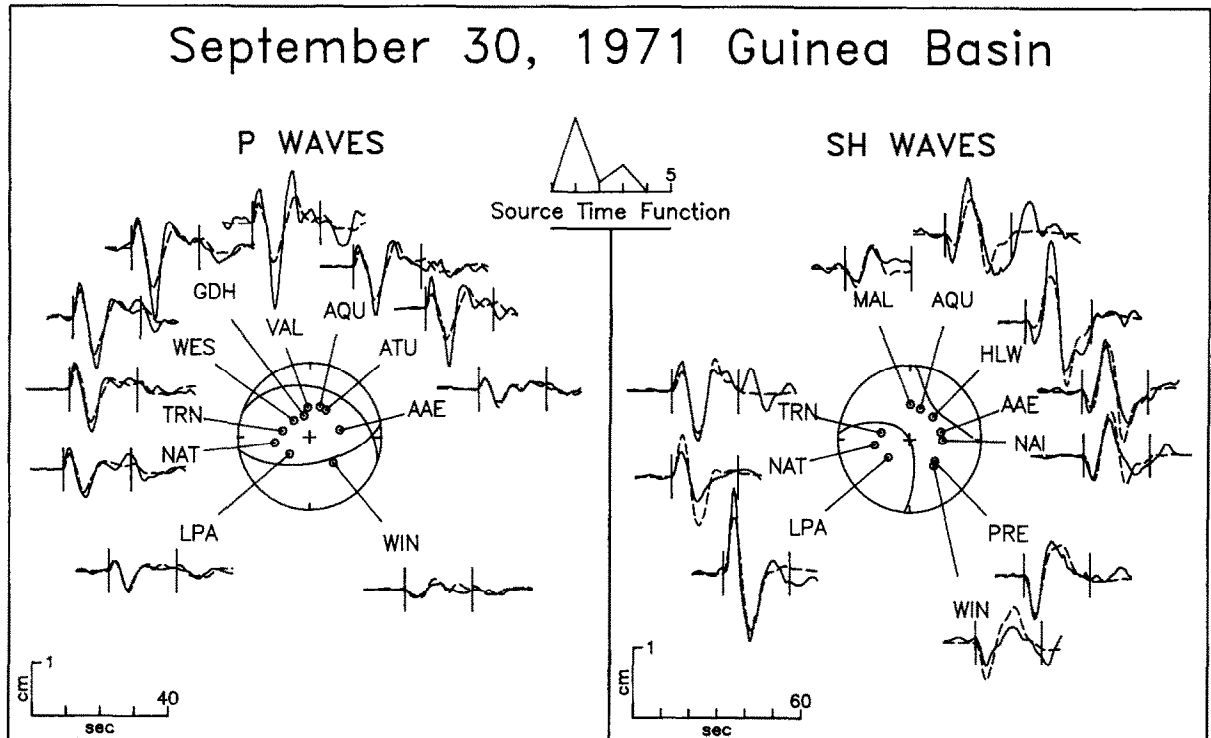


Fig. A5. Comparison of observed P and SH waves from the September 30, 1971 earthquake with synthetic waveforms generated for the best-fitting point source mechanism found in the body-waveform inversion. See Fig. A1 for further explanation.

is very similar to the time function reported by Liu and Kanamori, but the inversion requires some later release of energy and a total length of about 4 seconds.

May 21, 1972 (Figs. 9 and A6)

Bergman and Solomon (1980) presented first-motion polarities for the May 21, 1972 earthquake in the South Fiji Basin. Compressional first arrivals are consistently observed to the northwest, but the distribution is inadequate to completely constrain the focal mechanism. Wiens and Stein (1983) inferred a mechanism from these data and modeled P waveforms to estimate the depth of the May 1972 earthquake to be 10 km. The distribution of usable waveforms for this event, like the first motion data, is very poor. The SH waveform at KIP is very noisy and thus has little weight in the inversion, but the synthetic waveform matches well with the long-period character. The focal mechanism (333/71/157) is dominated by strike-

slip motion. The centroid depth is 13 km and the seismic moment is 4.7×10^{24} dyn cm.

October 20, 1972 (Figs. 3 and A7)

The source mechanism of the October 20, 1972, earthquake in the eastern Atlantic was first studied by Richardson and Solomon (1977), using P wave first motions and shear wave polarizations. The focal mechanism is characterized by nearly pure strike-slip motion (248/80/171). They also reported a seismic moment, estimated from long-period SH wave spectra, of 2.8×10^{25} dyn cm. From P-wave modeling, the depth of this event was estimated to be 20 km by Wiens and Stein (1983).

Station coverage for this event is exceptionally good; there are data in all four quadrants of both the P and SH radiation patterns. The vertical component instrument at LOR was found to have reversed polarity. With a mechanism (250/79/169) very close to that of Richardson and Solomon and

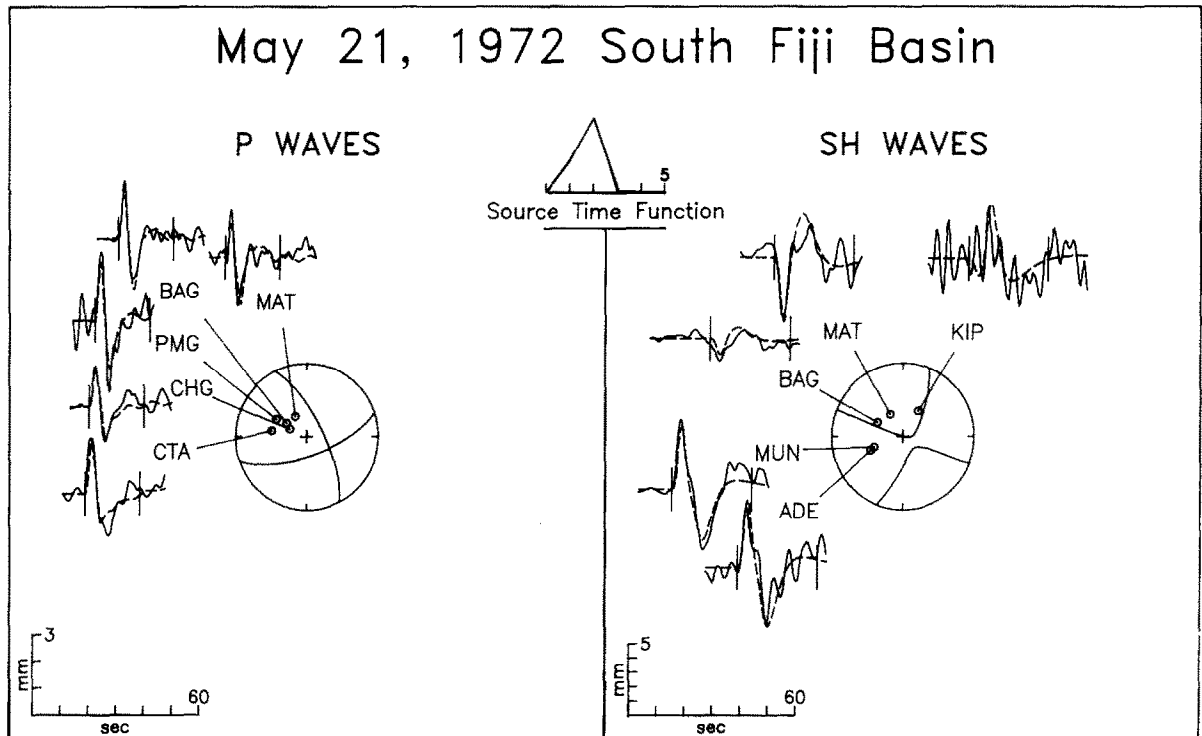


Fig. A6. Comparison of observed P and SH waves from the May 21, 1972 earthquake with synthetic waveforms generated for the best-fitting point source mechanism found in the body-waveform inversion. See Fig. A1 for further explanation.

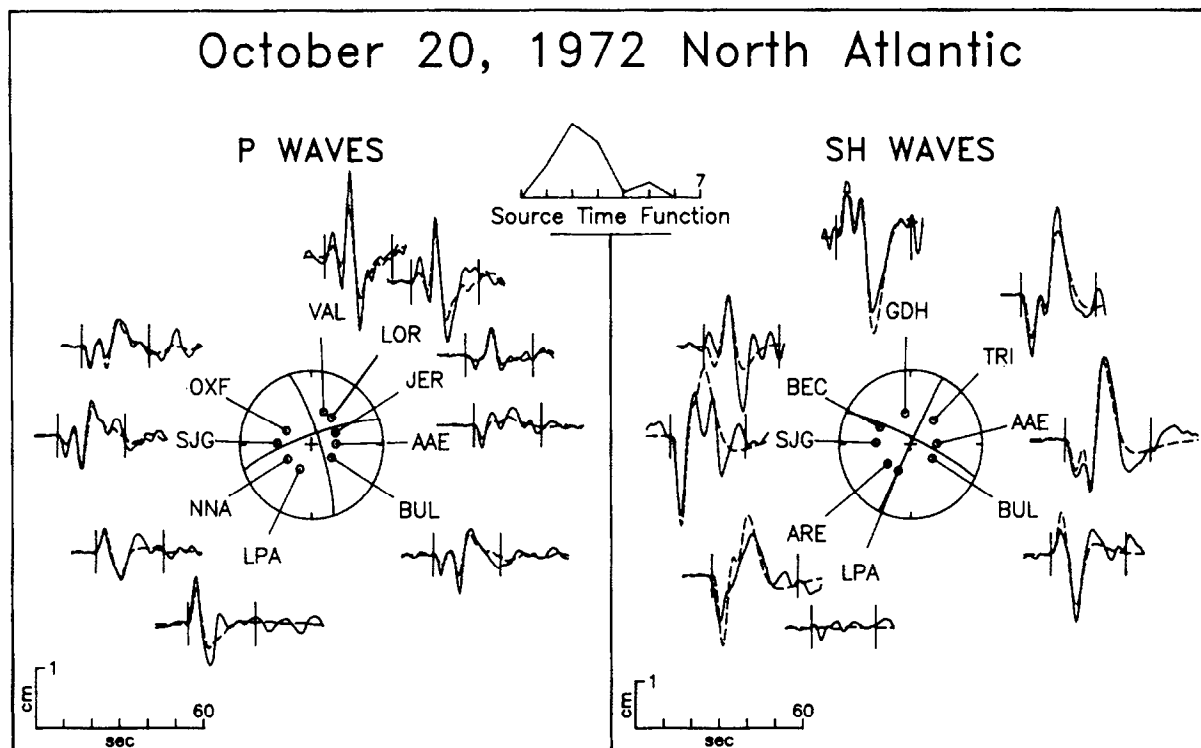


Fig. A7. Comparison of observed P and SH waves from the October 20, 1972 earthquake with synthetic waveforms generated for the best-fitting point source mechanism found in the body-waveform inversion. See Fig. A1 for further explanation.

a centroid depth of 18 km, the fit to the observed waveforms is quite good. Note that both the direct and reflected SH phases at LPA are nodal. The seismic moment found in the inversion (2.7×10^{25} dyn cm) is in excellent agreement with the estimate of Richardson and Solomon (1977).

April 26, 1973 (Figs. 10 and A8)

Unger and Ward (1979) made an extensive study of the location of the mainshock of the April 26, 1973 earthquake and its many aftershocks, using data from the local seismic array on Hawaii. They found a depth of 48 km for the mainshock (35–55 km for the aftershocks), making this one of the deepest known events in the interior of an oceanic plate. Supplementing the local seismic array data with first motion polarities at teleseismic stations, they proposed a predominantly strike-slip focal mechanism for this earthquake: 110/61/345.

Butler (1982) made an extensive body-wave

modeling study of the Hawaiian event, using P, SH, and SV waveforms in a trial-and-error approach and refining the model with a formal inversion of P and SH waveforms. Butler emphasizes the complex nature of the faulting in this earthquake and treats it as a double event. He was unable to find a mechanism for the first subevent which would satisfactorily fit both the P and SH waveforms, although his “1P” and “1S” mechanisms are not very different (0/94/141 and 351/81/152, respectively). The second subevent, located northeast of the first and delayed by several seconds, has a similar mechanism: 346/95/145. The depths of the two subevents are 42 and 32 km, respectively, and the total seismic moment is approximately 4.5×10^{25} dyn cm.

Butler’s mechanism is similar to, but rotated by 33° with respect to the mechanism proposed by Unger and Ward (1979). He explains both this discrepancy and the difference in depth by reference to the complicated and largely unknown velocity structure of Hawaii, which can have a

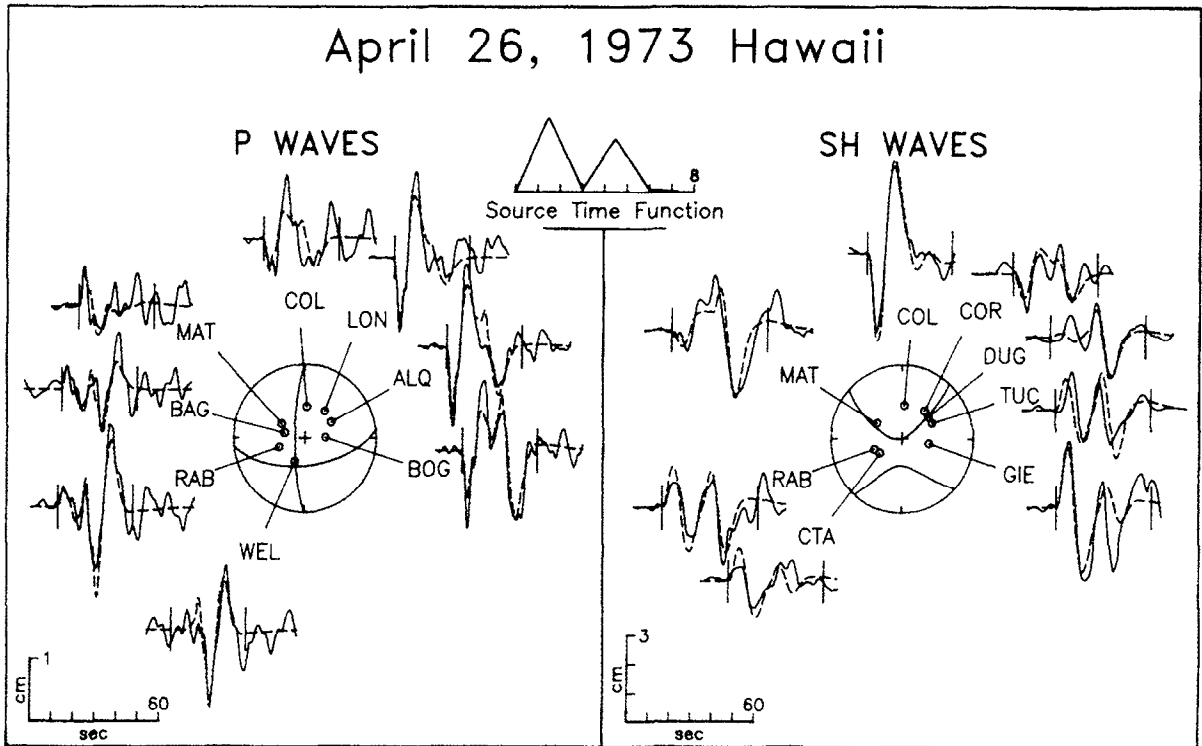


Fig. A8. Comparison of observed P and SH waves from the April 26, 1973 earthquake with synthetic waveforms generated for the best-fitting point source mechanism found in the body-waveform inversion. See Fig. A1 for further explanation.

severe effect on the travel paths to the local stations. Another factor in the depth discrepancy is that Unger and Ward's depth would correspond to the point at which faulting initiated, while the depth given by Butler would correspond to the centroid depth, or the approximate center of the ultimate fault area.

For the inversion study, I adapted the layered source structure of Butler (1982): the upper three layers are unmodified, but we approximated the lower part as a halfspace with $\alpha = 8.1$ km/s, $\beta = 4.7$ km/s, and $\rho = 3.4$ g/cm³. The 8 P and 8 SH waves selected for the inversion provide very good azimuthal coverage and the signal-to-noise ratio at most stations is excellent.

I investigated a number of parameterizations for this event, including multiple subevent models and horizontally-propagating point source models. Although some insight into the detailed rupture history of this event was gained (discussed below), the resolution of anything beyond an average point source solution is poor and none of these models

provided enough of an improvement in the fit to the observed waveforms to justify the added complexity. My preferred solution for this event is a single point source, with a mechanism of 83/59/347, quite similar to Butler's 1P solution. The centroid depth is 45 km, and the seismic moment is 4.6×10^{25} dyn cm. The source time function has two distinct pulses, which accounts satisfactorily for most of the complexity in the observed waveforms.

If these two pulses are treated as subevents in the inversion, solving for the source parameters of each, plus their relative timing and location, the solution differs little from the single-source model and the residual error is only slightly decreased. The depths of the two subevents are about 43 and 48 km and their mechanisms are nearly identical to the single-source model, except for strike. The first subevent has a strike of about N90E, while the second strikes nearer to N75E. The strike of our single event solution is an average of these two subevents. The second subevent is delayed by

about 3 s and located a short distance to the east or northeast. This solution corresponds well with the aftershock pattern (Fig. 11), leading to the conclusion that this event ruptured mainly from west to east, with a 20° – 30° counterclockwise rotation in strike in the eastern half.

April 12, 1974 (Figs. 12 and A9)

A strike-slip focal mechanism (274/76/180) for the April 12, 1974 Philippine Sea earthquake was reported by Bergman and Solomon (1980), based on first motion polarities. Wiens and Stein (1983) modeled P waves for this event, using this mechanism, and estimated the depth to be 7 km below the seafloor. Because of the small size of this event and its location, the number of stations with usable waveform data is small and the distribution of stations is very poor. Even so, the available P and SH waveform data are incompatible with the strike-slip mechanism of Bergman and Solomon (1980). The preferred mechanism is characterized by thrust faulting on nodal planes striking roughly

E–W (72/53/71). The seismic moment is quite small, 1.2×10^{24} dyn cm, and the centroid depth is 11 km.

November 20, 1974 (Figs. 6 and A10)

Wiens and Stein (1983) proposed a strike-slip mechanism (275/82/5) and a depth of 8 km for the November 20, 1974 earthquake in the South Atlantic, based on first motion polarities and P waveform modeling. Waveform data suitable for the inversion were recorded at only a few stations, but they are fairly well distributed. I investigated strike-slip mechanisms for this event, but obtained a more satisfactory fit to the waveforms, particularly the P waves, with a predominantly thrust-faulting mechanism (333/46/69). The starting points for the P waves were established by referring to the short-period P waveforms, which are extremely clear in most cases. There is some evidence that this event ruptured in several pulses, perhaps with rather different mechanisms, but the data are inadequate to resolve such details. The

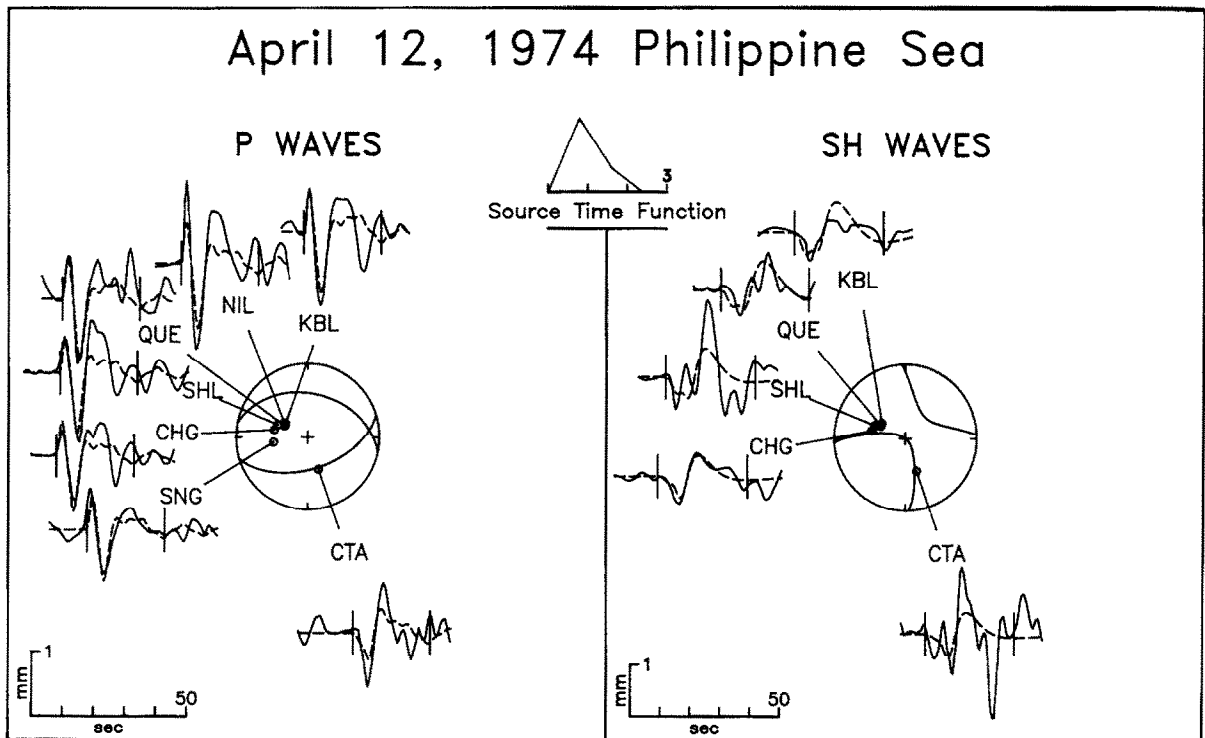


Fig. A9. Comparison of observed P and SH waves from the April 12, 1974 earthquake with synthetic waveforms generated for the best-fitting point source mechanism found in the body-waveform inversion. See Fig. A1 for further explanation.

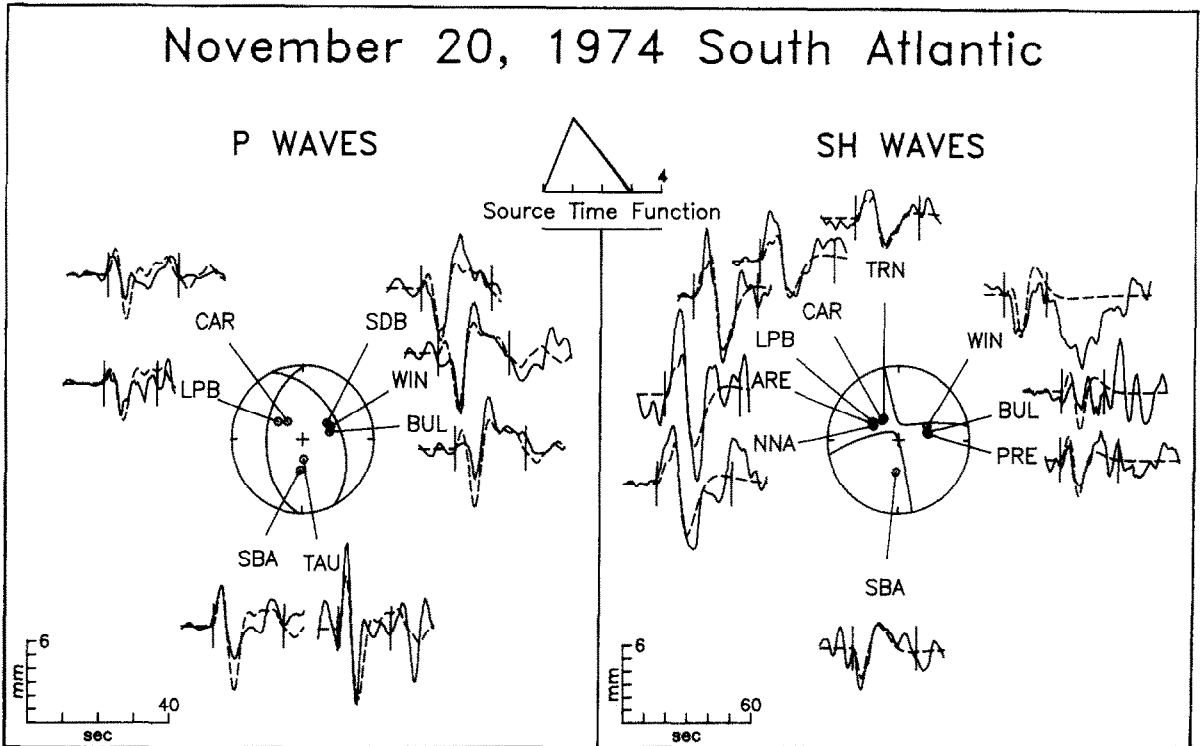


Fig. A10. Comparison of observed P and SH waves from the November 20, 1974 earthquake with synthetic waveforms generated for the best-fitting point source mechanism found in the body-waveform inversion. See Fig. A1 for further explanation.

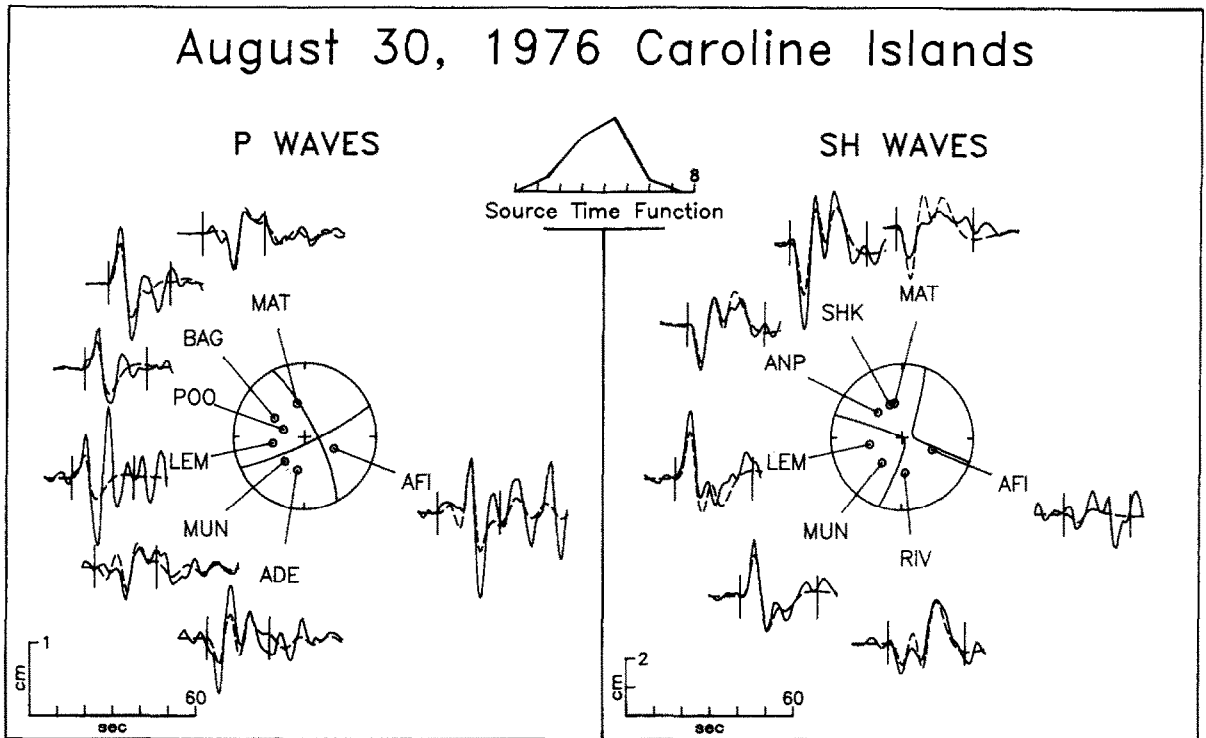


Fig. A11. Comparison of observed P and SH waves from the August 30, 1976 earthquake with synthetic waveforms generated for the best-fitting point source mechanism found in the body-waveform inversion. See Fig. A1 for further explanation.

best-fitting centroid depth is 11 km. The seismic moment is estimated to be 7.2×10^{24} dyn cm.

August 30, 1976 (Figs. 7 and A11)

Both Hegarty et al. (1983) and Wiens and Stein (1983) reported source mechanisms, based on first motions and waveform modeling (both P and SH waves in the case of Hegarty et al.), for the August 30, 1976 earthquake in the Caroline Islands. The focal mechanisms are quite similar, but the source depths differ somewhat: Hegarty et al. give a mechanism of 330/69/175, a depth of 20 km, and a seismic moment of 1.5×10^{25} dyn cm, while Wiens and Stein's mechanism is 338/77/180, with a depth of 28 km.

This earthquake was very well recorded; clear P and SH waveform data cover an azimuthal range of 270° . The focal mechanism found in the inversion (332/76/172) is close to those noted above. The centroid depth is 26 km. The solution is dominated by the SH waves; no simple source was found which gives a good fit to all the P wave-

forms simultaneously. The depth signature in the SH waves for this event is remarkably clear at several stations (e.g., RIV, ANP, and SHK) and I suspect that the greater depth reported by Wiens and Stein is the result of using only P waveforms. When P waveforms alone were used in the inversion, the best-fitting centroid depth was several kilometers deeper. The seismic moment found in the inversion (2.5×10^{25} dyn cm) is somewhat larger than the estimate of Hegarty et al.

February 5, 1977 (Figs. 13 and A12)

Bergman and Solomon (1980) noted that all teleseismic first motions for the February 5, 1977 earthquake in the southeast Pacific are compressional, indicating a thrust faulting mechanism, but the first motion data provide no constraint on the strike of the nodal planes. Using surface wave radiation patterns, Okal (1980) determined that the mechanism involved thrust faulting on planes striking nearly N-S (1/58/82). He also reported a seismic moment of 4.4×10^{25} dyn cm and a depth

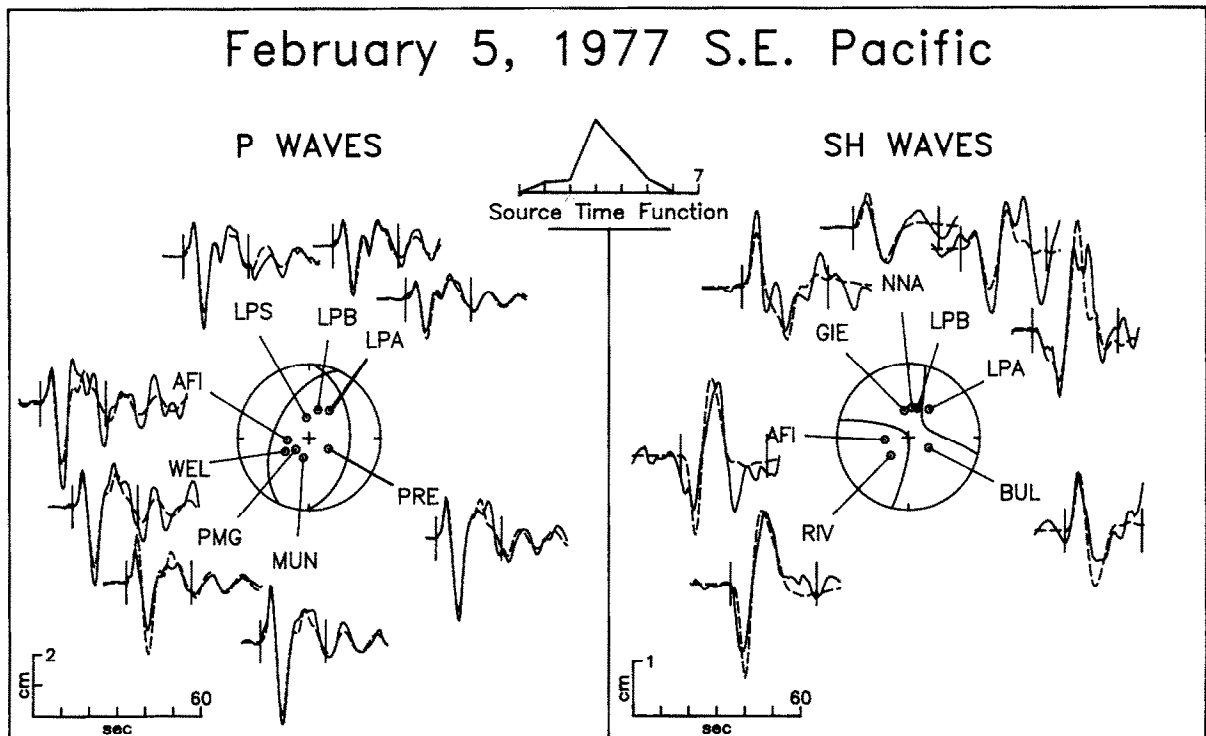


Fig. A12. Comparison of observed P and SH waves from the February 5, 1977 earthquake with synthetic waveforms generated for the best-fitting point source mechanism found in the body-waveform inversion. See Fig. A1 for further explanation.

of 35 km, based on the ratio of amplitudes of Love and Rayleigh waves. Wiens and Stein (1983) reported a depth of 15 km, however, based on P wave modeling.

The source structure for the inversion included a 1.4 km thick sediment layer (Houtz, 1974) with $\alpha = 2.0$ km/s, $\beta = 0.8$ km/s, and $\rho = 2.0$ g/cm³. The distribution of stations at which clear P and SH waveforms were recorded is quite good and the inversion quickly converged to a mechanism very similar to that of Okal (2/42/73), with a seismic moment of 3.9×10^{25} dyn cm and a centroid depth of 15 km below the seafloor. The source time function has a small initial pulse, followed by the main rupture.

October 17, 1977 (Figs. 9 and A13)

Because of its magnitude, most of the shear waves recorded for the October 17, 1977 earthquake in the South Fiji Basin were clipped or too faint to digitize; only three usable SH waveforms were obtained. Many of the P waveforms are quite

complex and variable between neighboring stations, presumably the result of source finiteness. For the point source inversion, I selected a small but well-distributed set of the simplest P waveforms. The focal mechanism of this event is well constrained, even by the small set of data used here, to be a predominantly strike-slip mechanism (274/78/9). The seismic moment is 2.0×10^{26} dyn cm, making this one of the largest known oceanic intraplate earthquakes, and the centroid depth is 13 km.

The P waveforms which show the most complexity are those located nearest to the nodal planes; they are probably influenced more by directivity in the rupture propagation than by any intrinsic complexity (e.g., multiple rupture or changes in mechanism) in the rupture history of this earthquake. The source time function is 7.5 s in duration and remarkably simple. Because of the paucity of SH wave data, no attempt was made to infer the fault plane for this event by using a horizontally-propagating point source model.

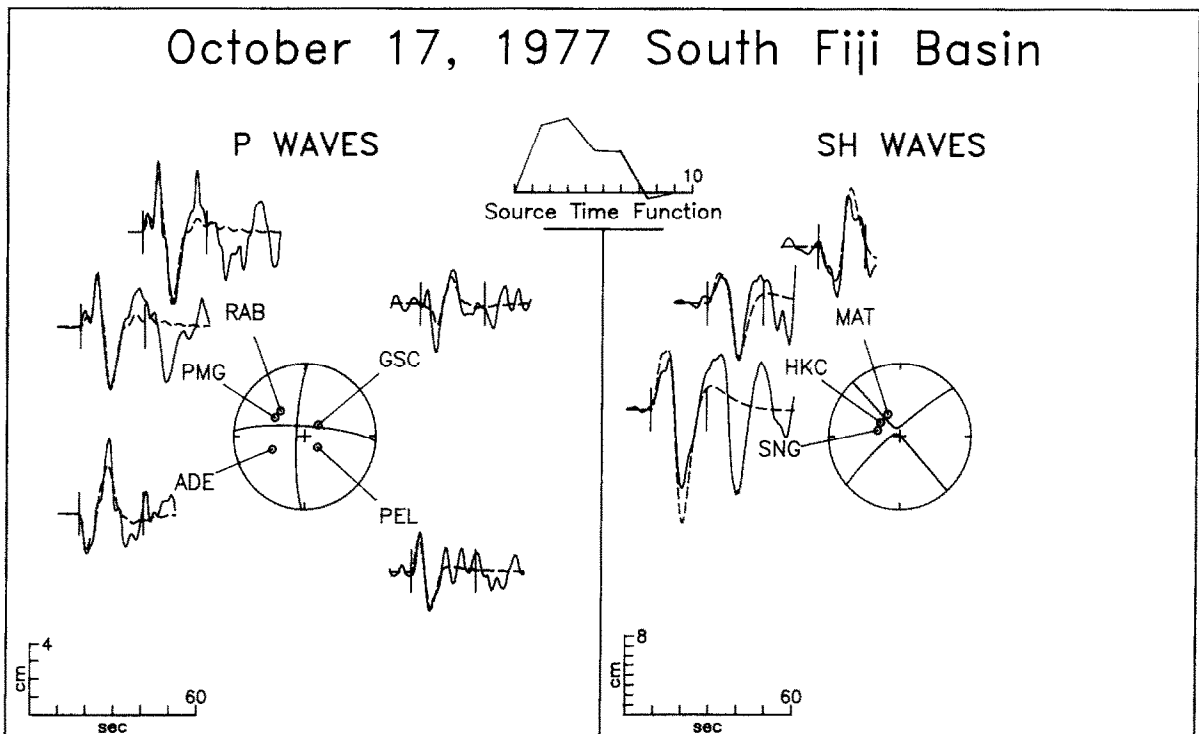


Fig. A13. Comparison of observed P and SH waves from the October 17, 1977 earthquake with synthetic waveforms generated for the best-fitting point source mechanism found in the body-waveform inversion. See Fig. A1 for further explanation.

December 13, 1977 (Figs. 5 and A14)

Bergman and Solomon (1980) studied the December 13, 1977 earthquake using first motion polarities and shear wave polarization, finding a strike-slip mechanism with a component of thrust faulting (238/72/38). Stein et al. (1982) modeled the P waveforms and found a similar mechanism, but with a larger component of thrust faulting (244/68/65). They found a depth of 25 km and a seismic moment (from surface waves) of 5.4×10^{25} dyn cm. As expected for a large event in the central Atlantic, the station coverage is excellent. The fit to the observed waveforms is very good with a mechanism intermediate between the two previously published solutions: 238/60/49. The centroid depth is 20 km, somewhat shallower than the depth reported by Stein et al., and the seismic moment is 4.5×10^{25} dyn cm. The source time function has an initial pulse about 3 s in duration, followed by a lower level of moment release for several more seconds.

March 24 1978 (Figs. 4 and A15)

Stewart and Helmberger (1981) modeled P and SH waveforms from the Bermuda Rise earthquake of March 24, 1978 and reported the best-fitting mechanism to be 340/42/90, with a seismic moment of 3.4×10^{25} dyn cm and a depth of about 6 km below the seafloor. A seismic moment of 3.1×10^{25} dyn cm was estimated from long-period Rayleigh waves recorded by the IDA network. Nishenko and Kafka (1982) studied the source mechanism with first motion data and Rayleigh wave amplitude spectra, finding a mechanism (340/55/90) nearly identical to that of Stewart and Helmberger, a seismic moment of 3.6×10^{25} dyn cm, and an identical depth of 6 km.

The source structure used in the body-waveform inversion incorporated a 1.2 km thick sediment layer (Ewing et al., 1954), with $\alpha = 2.0$ km/s, $\beta = 0.8$ km/s, and $\rho = 2.3$ g/cm³. Station coverage for this event is quite good in the northern hemisphere, but poor in the south. The focal

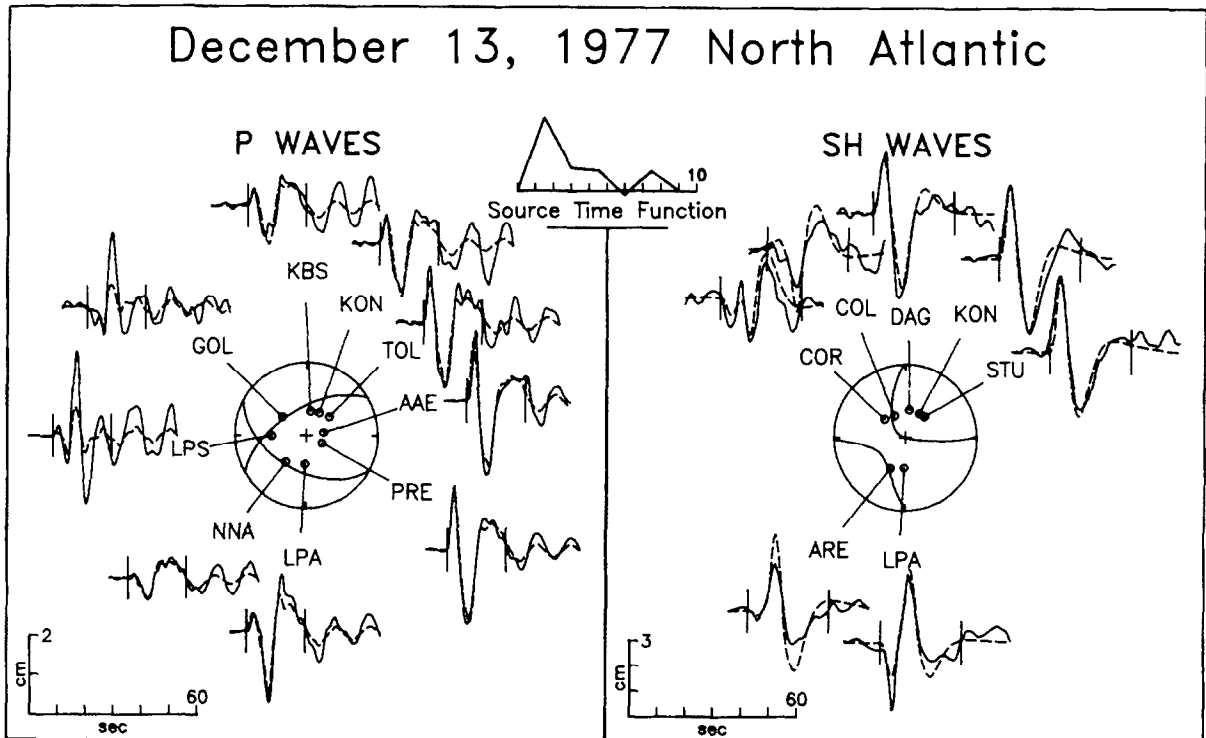


Fig. A14. Comparison of observed P and SH waves from the December 13, 1977 earthquake with synthetic waveforms generated for the best-fitting point source mechanism found in the body-waveform inversion. See Fig. A1 for further explanation.

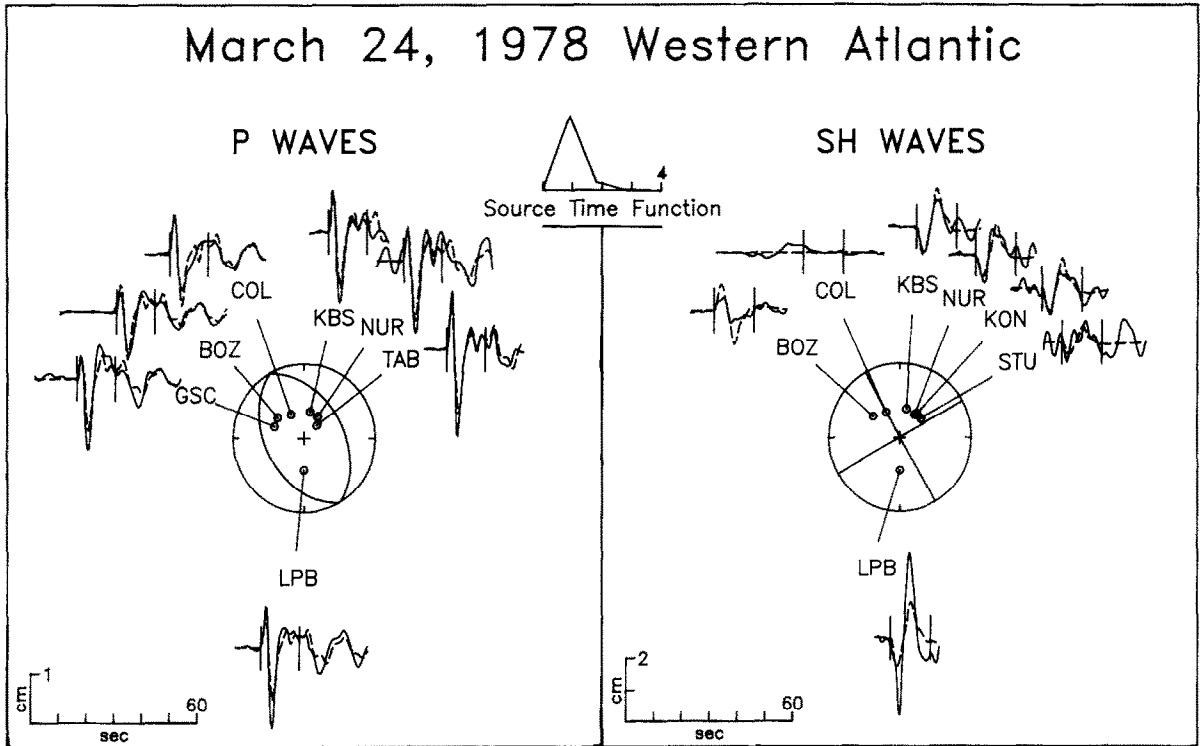


Fig. A15. Comparison of observed P and SH waves from the March 24, 1978 earthquake with synthetic waveforms generated for the best-fitting point source mechanism found in the body-waveform inversion. See Fig. A1 for further explanation.

mechanism (330/44/89) is well constrained by the SH wave data. There are stations in three quadrants of the SH radiation pattern and both the direct and reflected SH phases at COL are nodal, which limits the range of acceptable fault strike. The centroid depth found in the inversion (8 km) is slightly deeper than previous estimates and the seismic moment (2.2×10^{25} dyn cm) is somewhat smaller. The source time function is unusually short (2 s) for an event of this size, suggesting a relatively high average stress drop.

Acknowledgements

I thank Sean Solomon for many enlightening discussions concerning this research, and for a critical reading of any early version of the manuscript. I also thank Doug Wiens and an anonymous reviewer for helpful comments. Linda Meinke provided data on isochrons in oceanic lithosphere and assisted with figure preparation. I thank Jan Nattier-Barbaro for help with manu-

script preparation. This research was supported by the National Aeronautics and Space Administration under contract NAS 5-27339 and the National Science Foundation under grant EAR-8416192.

References

- Aki, K. and Richards, P.G., 1980. *Quantitative Seismology: Theory and Methods*, Vol. 1. Freeman, San Francisco, Calif., 557 pp.
- Ball, M.M. and Harrison, C.G., 1970. Crustal plates in the central Atlantic. *Science*, 167: 1128–1129.
- Barker, P.F., 1972. A spreading centre in the east Scotia Sea. *Earth Planet. Sci. Lett.*, 15: 123–132.
- Barker, P.F. 1982. A Cenozoic subduction history of the Pacific margin of the Antarctic Peninsula: ridge crest–trench interactions. *J. Geol. Soc. London*, 139: 787–801.
- Bergman, E.A., 1984. Intraplate earthquakes and the state of stress in oceanic lithosphere. Ph.D. Thesis, Mass. Inst. Technol., Cambridge, Mass., 438 pp.
- Bergman, E.A. and Solomon, S.C., 1980 Oceanic intraplate earthquakes: implications for local and regional intraplate stress. *J. Geophys. Res.*, 85: 5389–5410.

- Bergman, E.A. and Solomon, S.C., 1984. Source mechanisms of earthquakes near mid-ocean ridges from body waveform inversion: implications for the early evolution of oceanic lithosphere. *J. Geophys. Res.*, 89: 11415–11441.
- Bergman, E.A. and Solomon, S.C., 1985. Earthquake source mechanisms from body-waveform inversion and intraplate tectonics in the northern Indian Ocean. *Phys. Earth Planet. Inter.*, 40: 1–23.
- Bergman, E.A., Nabelek, J.L. and Solomon, S.C., 1984. An extensive region of off-ridge normal-faulting earthquakes in the southern Indian Ocean. *J. Geophys. Res.*, 89: 2425–2443.
- Bergman, E.A., Nabelek, J.L. and Solomon, S.C., 1985. Correction to “An extensive region of off-ridge normal-faulting earthquakes in the southern Indian Ocean” by E.A. Bergman, J.L. Nabelek and S.C. Solomon. *J. Geophys. Res.*, 90: 2066–2067.
- Brace, D.R., 1975. Reconnaissance geophysical survey of the Caroline Basin. *Geol. Soc. Am. Bull.*, 86: 775–784.
- Bratt, S.R., Bergman, E.A. and Solomon, S.C., 1985. Thermoelastic stress; How important as a cause of earthquakes in young oceanic lithosphere? *J. Geophys. Res.*, 90: 10249–10260.
- Brotchie, J.F., 1971. Flexure of a liquid-filled spherical shell in a radial gravity field. *Modern Geol.*, 3: 15–23.
- Butler, R., 1982. The 1973 Hawaii earthquake: a double earthquake beneath the volcano Mauna Kea. *Geophys. J. R. Astron. Soc.*, 69: 173–186.
- Cande, S.C., Herron, E.M. and Hall, B.R., 1982. The early Cenozoic tectonic history of the southeast Pacific. *Earth Planet. Sci. Lett.*, 57: 63–74.
- Chase, C.G., 1978. Plate kinematics: the Americas, East Africa, and the rest of the world. *Earth Planet. Sci. Lett.*, 37: 355–368.
- Chen, W.-P. and Molnar, P., 1983. Focal depths of intracontinental and intraplate earthquakes and their implications for the thermal and mechanical properties of the lithosphere. *J. Geophys. Res.*, 88: 4183–4215.
- Cloetingh, S. and Wortel, R., 1985. Regional stress field of the Indian plate. *Geophys. Res. Lett.*, 12: 77–80.
- Craddock, C., 1981. Plate-Tectonic Map of the Circum-Pacific Region, Antarctic Panel. Am. Assoc. Pet. Geol., Tulsa, Okla.
- Dahlen, F.A., 1981. Isostasy and the ambient state of stress in the oceanic lithosphere. *J. Geophys. Res.*, 86: 7801–7807.
- Drummond, K.J., 1981. Plate-Tectonic Map of the Circum-Pacific Region, Northeast Quadrant. Am. Assoc. Pet. Geol., Tulsa, Okla.
- Eaton, J.P., 1962. Crustal structure and volcanism in Hawaii. In: G.A. Macdonald and H. Kuno (Editors), *The Crust of the Pacific Basin*. Geophys. Monogr., Am. Geophys. Union, Vol. 6, pp. 13–29.
- Ewing, M., Sutton, G.H. and Officer, C.B., 1954. Seismic refraction measurements in the Atlantic Ocean, VI. Typical deep stations, North American Basin. *Bull. Seismol. Soc. Am.*, 44: 21–38.
- Fiske, R.S. and Jackson, E.D., 1972. Orientation and growth of Hawaiian rifts: The effect of regional structure and gravitational stresses. *Proc. R. Soc. London*, 329: 299–326.
- Fitch, T.J., 1981. Correction and addition to “Estimation of the seismic moment tensor from teleseismic body wave data with applications to intraplate and mantle earthquakes” by T.J. Fitch, D.W. McCowan, and M. W. Shields. *J. Geophys. Res.*, 86: 9375–9376.
- Forsyth, D.W., 1975. Fault plane solutions and tectonics of the south Atlantic and Scotia Sea. *J. Geophys. Res.*, 80: 1429–1443.
- Green, D.H., 1971. Composition of basaltic magmas as indicators on conditions of origin: applications to oceanic volcanism. *Philos. Trans. R. Soc. London, Ser. A*, 268: 707–725.
- Hegarty, K.A., Weissel, J.K. and Hayes, D.E., 1983. Convergence at the Caroline–Pacific plate boundary: collision and subduction. In: D.E. Hayes (Editor), *The Tectonic and Geologic Evolution of Southeast Asian Seas and Islands*, Part 2, Geophys. Monogr., Am. Geophys. Union, Vol. 27, pp. 326–348.
- Hilde, T.W.C. and Lee, C.-S., 1984. Origin and evolution of the west Philippine Basin: a new interpretation. *Tectonophysics*, 102: 85–104.
- Houtz, R.E., 1974. Continental margin of Antarctica: Pacific–India sectors. In: C.A. Burk and C.L. Drake (Editors), *The Geology of Continental Margins*. Springer, New York, N.Y., pp. 655–658.
- Jackson, E.D. and Shaw, H.R., 1975. Stress fields in the central portions of the Pacific plate: delineated in time by linear volcanic chains. *J. Geophys. Res.*, 80: 1861–1874.
- Jackson, E.D., Silver, E.A. and Dalrymple, G.B., 1972. Hawaiian–Emperor chain and its relation to Cenozoic circum-Pacific tectonics. *Geol. Soc. Am. Bull.*, 83: 601–617.
- Karig, D.E., 1971. Origin and development of marginal basins in the western Pacific. *J. Geophys. Res.*, 76: 2542–2561.
- Koyanagi, R.Y., Swanson, D.A. and Endo, E.T., 1972. Distribution of earthquakes related to mobility of the south flank of Kilauea Volcano, Hawaii. *U.S. Geol. Surv., Prof. Pap.*, 800-D: D89–D97.
- LaBrecque, J.L. and Rabinowitz, P.D., 1981. General Bathymetric Chart of the Oceans (GEBCO), Sheet 5.16, 5th Ed. Canadian Hydrographic Service, Ottawa.
- LaBrecque, J.L., Kent, D.V. and Cande, S.C., 1977. Revised magnetic polarity time scale for Late Cretaceous and Cenozoic time. *Geology*, 5: 330–335.
- Lay, T. and Okal, E.A., 1983. The Gilbert Islands (Republic of Kiribati) earthquake swarm of 1981–83. *Phys. Earth Planet. Inter.*, 33: 284–303.
- Lilwall, R.C., 1982. Intraplate seismicity and seismic risk in the Atlantic Ocean based on teleseismically observed earthquakes. *Inst. of Oceanogr., Sci. Rep.*, 136, 43 pp.
- Liu, H.-L. and Kanamori, H., 1980. Determination of source parameters of midplate earthquakes from the wave forms of body waves. *Bull. Seismol. Soc. Am.*, 70: 1989–2004.
- Mammerickx, J., 1978. Re-evaluation of some geophysical ob-

- servations in the Caroline basins. *Geol. Soc. Am. Bull.*, 89: 192–196.
- McKenzie, D.P., 1969. The relation between fault plane solutions for earthquakes and the directions of principal stresses. *Bull. Seismol. Soc. Am.*, 59: 591–601.
- Minster, J.B. and Jordan, T.H., 1978. Present-day plate motions. *J. Geophys. Res.*, 83: 5331–5354.
- Minster, J.B., Jordan, T.H., Molnar, P. and Haines, E., 1974. Numerical modelling of instantaneous plate tectonics. *Geophys. J. R. Astron. Soc.*, 36: 541–576.
- Molnar, P. and Sykes, L.R., 1969. Tectonics of the Caribbean and Middle America regions from focal mechanisms and seismicity. *Geol. Soc. Am. Bull.*, 80: 1639–1684.
- Nabelek, J.L., 1984. Determination of earthquake source parameters from inversion of body waves. Ph.D. Thesis, Mass. Inst. Technol., Cambridge, Mass., 361 pp.
- Newmark, R.L., Zoback, M.D. and Anderson, R.N., 1984. Orientation of in-situ stresses near the Costa Rica rift and the Peru-Chile trench: DSDP hole 504B. *Nature*, 311: 424–428.
- Nishenko, S.P. and Kafka, A.F., 1982. Earthquake focal mechanisms and the intraplate setting of the Bermuda Rise. *J. Geophys. Res.*, 87: 3929–3941.
- Nishenko, S.P., Purdy, G.M. and Ewing, J.I., 1982. Micro-aftershock survey of the 1978 Bermuda Rise earthquake. *J. Geophys. Res.*, 87: 10624–10636.
- Nishiwaki, C., 1981. Plate-Tectonic Map of the Circum-Pacific Region, Northwest Quadrant. *Am. Assoc. Pet. Geol.*, Tulsa, Okla.
- Okal, E.A., 1980. The Bellingshausen Sea earthquake of February 5, 1977: evidence for ridge-generated compression in the Antarctic plate. *Earth Planet. Sci. Lett.*, 46: 306–310.
- Okal, E.A., 1984. Intraplate seismicity of the southern part of the Pacific plate. *J. Geophys. Res.*, 89: 10053–10071.
- Okal, E.A., Talandier, J., Sverdrup, K.A. and Jordan, T.H., 1980. Seismicity and tectonic stress in the South-Central Pacific. *J. Geophys. Res.*, 85: 6479–6495.
- Parsons, B. and Sclater, J.G., 1977. An analysis of the variation of ocean floor bathymetry and heat flow with age. *J. Geophys. Res.*, 82: 803–827.
- Perry, R.K., Fleming, H.S. and Vogt, P.R., 1981. North Atlantic Ocean: bathymetry and Plate Tectonic Evolution (Map). Acoustics Div., Acoustic Media Characterization Branch, Naval Res. Lab., Washington, D.C.
- Poppe, B.B., Naab, D.A. and Perry, J.S., 1978. Seismograph station codes and characteristics. *U.S. Geol. Surv., Circ.* 791, 171 pp.
- Raleigh, C.B., Healy, J.H. and Bredehoeft, J.D., 1972. Faulting and crustal stress at Rangely, Colorado. In: H.C. Heard, I.Y. Borg, N.L. Carter and C.B. Raleigh (Editors), *Flow and Fracture of Rocks*. *Geophys. Monogr.*, Am. Geophys. Union, Vol. 16, pp. 275–284.
- Richardson, R.M., 1983. Inversion for the plate driving forces of plate tectonics. In: *Proceedings of the International Geoscience Remote Sensing Symposium*, Vol. II. Inst. of Electr. and Electron. Eng., New York, pp. FA2.3.1–FA2.3.6.
- Richardson, R.M. and Cox, B.L., 1984. Evolution of oceanic lithosphere: a driving force study of the Nazca plate. *J. Geophys. Res.*, 89: 10043–10052.
- Richardson, R.M. and Solomon, S.C., 1977. Apparent stress and stress drop for intraplate earthquakes and tectonic stress in the plates. *Pure Appl. Geophys.*, 115: 317–331.
- Richardson, R.M., Solomon, S.C. and Sleep, N.H., 1979. Tectonic stress in the plates. *Rev. Geophys. Space Phys.*, 17: 981–1019.
- Rogers, D.B. and Endo, E.T., 1977. Focal mechanisms for upper mantle earthquakes and flexure of the lithosphere near Hawaii (abstr.). *Eos, Trans. Am. Geophys. Union*, 58: 1231.
- Sandwell, D. and Schubert, G., 1982. Lithospheric flexure at fracture zones. *J. Geophys. Res.*, 87: 4657–4667.
- Sclater, J.G., Jaupart, C. and Galson, D., 1980. The heat flow through oceanic and continental crust and the heat loss of the Earth. *Rev. Geophys. Space Phys.*, 18: 269–311.
- Sclater, J.G., Parsons, B. and Jaupart, C., 1981. Oceans and continents: similarities and differences in the mechanisms of heat loss. *J. Geophys. Res.*, 86: 11535–11552.
- Sibuet, J.-C. and Mascle, J., 1978. Plate kinematic implications of Atlantic equatorial fracture zone trends. *J. Geophys. Res.*, 83: 3401–3421.
- Stein, S., Engeln, J., Wiens, D., Fujita, K. and Speed, R., 1982. Subduction seismicity and tectonics in the Lesser Antilles Arc. *J. Geophys. Res.*, 87: 8642–8664.
- Stewart, G.S. and Helmberger, D.V., 1981. The Bermuda earthquake of March 24, 1978: a significant oceanic intraplate event. *J. Geophys. Res.*, 86: 7027–7036.
- Suyenaga, W., 1979. Isostasy and flexure of the lithosphere under the Hawaiian Islands. *J. Geophys. Res.*, 84: 5599–5604.
- Sykes, L.R. and Sbar, M.L., 1974. Focal mechanism solutions of intraplate earthquakes and stresses in the lithosphere. In: L. Kristjansson (Editor), *Geodynamics of Iceland and the North Atlantic Area*. Reidel, Hingham, Mass., pp. 207–224.
- Taylor, B. and Hayes, D.E., 1983. Origin and history of the South China Basin. In: D.E. Hayes (Editor), *The Tectonic and Geologic Evolution of Southeast Asian Seas and Islands*, Part 2. *Geophys. Monogr.*, Am. Geophys. Union, Vol. 27, pp. 23–56.
- Turcotte, D.L. and Oxburgh, E.R., 1973. Mid-plate tectonics. *Nature*, 244: 337–339.
- Unger, J.D. and Ward, P.L., 1979. A large deep Hawaiian earthquake—The Honoumuli, Hawaii event of April 26, 1973. *Bull. Seismol. Soc. Am.*, 69: 1771–1781.
- Walker, D.A. and McCreery, C.S., 1985. Significant unreported earthquakes in “aseismic” regions of the western Pacific. *Geophys. Res. Lett.*, 12: 433–436.
- Wang, S.-C., Geller, R.J., Stein, S. and Taylor, B., 1979. An intraplate thrust faulting earthquake in the South China Sea. *J. Geophys. Res.*, 84: 5627–5631.
- Watts, A.B., Weisell, J.K. and Davey, F.J., 1977. Tectonic evolution of the South Fiji marginal basin. In: M. Talwani and W.C. Pitman III (Editors), *Island Arcs, Deep Sea Trenches, and Back-Arc Basins*. Maurice Ewing Ser., Vol.

1. American Geophysical Union, Washington, D.C., pp. 419–428.
- Weissel, J.K. and Anderson, R.N., 1978. Is there a Caroline plate? *Earth Planet. Sci. Lett.*, 41: 143–158.
- Weissel, J.K., Hayes, D.E. and Herron, E.M., 1977. Plate tectonic synthesis: the displacements between Australia, New Zealand, and Antarctica since the late Cretaceous. *Mar. Geol.*, 25: 231–277.
- Wiens, D.A., 1986. Historical seismicity near Chagos: a complex deformation zone in the equatorial Indian Ocean. *Earth Planet. Sci. Lett.*, 76: 350–360.
- Wiens, D.A. and Stein, S., 1983. Age dependence of oceanic intraplate seismicity and implications for lithospheric evolution. *J. Geophys. Res.*, 88: 6455–6468.
- Wiens, D.A. and Stein, S., 1984. Intraplate seismicity and stresses in young oceanic lithosphere. *J. Geophys. Res.*, 89: 11442–11464.
- Wiens, D.A., DeMets, C., Gordon, R.G., Stein, S., Argus, D., Engeln, J.F., Lundgren, P., Quible, D., Stein, C., Weinstein, S. and Woods, D.F., 1985. A diffuse plate boundary model for Indian Ocean tectonics. *Geophys. Res. Lett.*, 12: 429–432.
- Zoback, M.D. and Zoback, M.L., 1980. State of stress in the conterminous United States. *J. Geophys. Res.*, 85: 6113–6156.